ISSN: 1810-2093

FJJM Fu-Jen Journal of Medicine

Vol. 23, No.3, September 2025

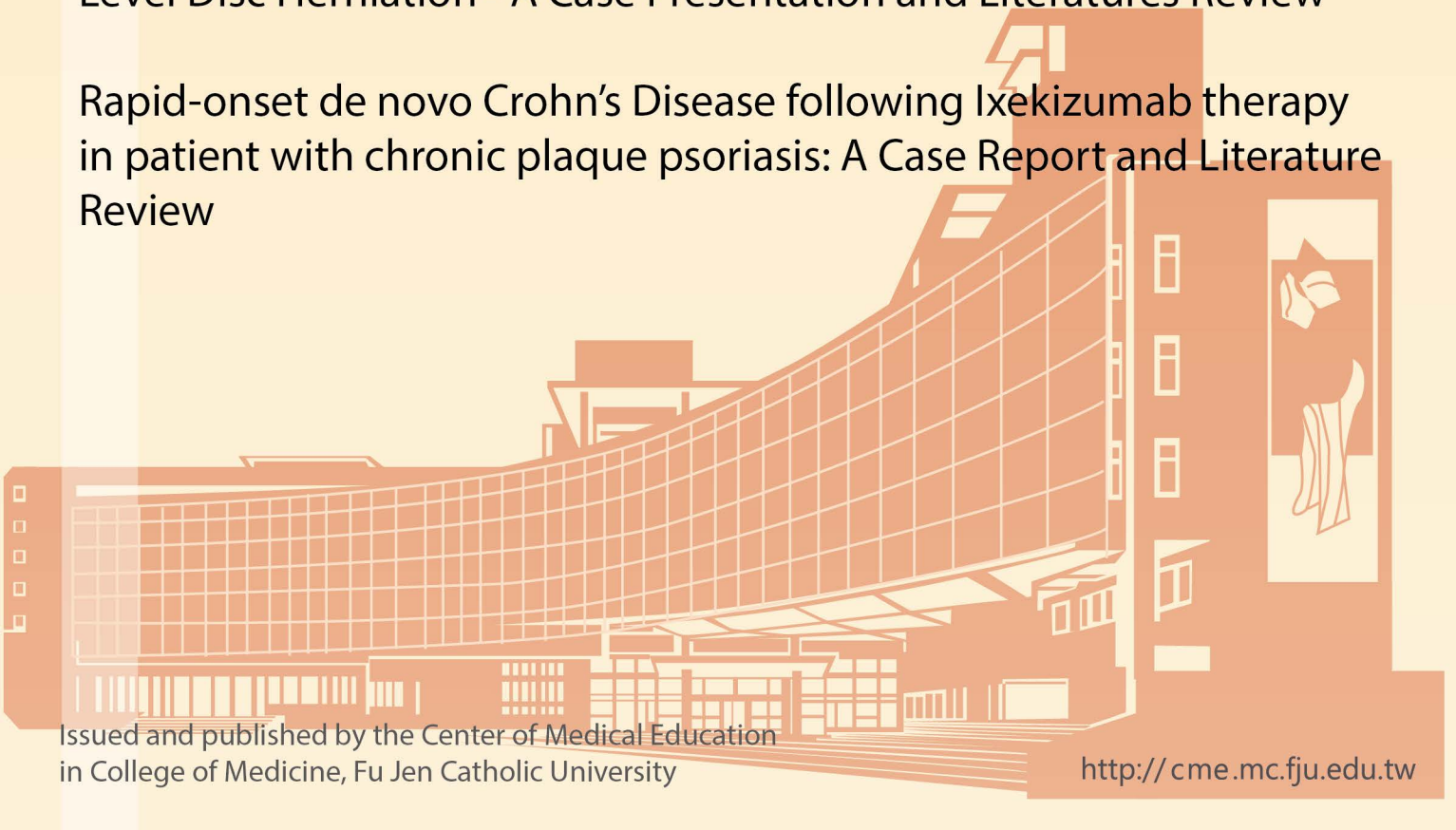

Issued and published by the Center of Medical Education
in College of Medicine, Fu Jen Catholic University

http:// cme.mc.fju.edu.tw

Fu-Jen Journal of Medicine

Vol. 23, No. 3, September 2025

CONTENTS

Original Research Article

Case Report

Submitted April 29, 2025.
Final version accepted May 20, 2025.

Cite as: Wan-Lun Hsu, Yukiko Ono, Zhi-Yi Lee, Shiou-Cheng Hu, Noi Yar, Ya Ker Huang, Chung-Kuan Wu
Moderate to severe mitral regurgitation affects major adverse cardiovascular outcomes and mortality among chronic hemodialysis patients
Fu-Jen Journal of Medicine 23(3): 1-17, 2025.
DOI: 10.53106/181020932025092303001

Original Research Article

Moderate to severe mitral regurgitation affects major adverse cardiovascular outcomes and mortality among chronic hemodialysis patients

Wan-Lun Hsu[1,2], Yukiko Ono[2], Zhi-Yi Lee[3], Shiou-Cheng Hu[3], Noi Yar[4], Ya Ker Huang[4], and Chung-Kuan Wu [3,4,5*]

[1] Master Program of Big Data Analysis in Medical Healthcare Industry, College of Medicine, Fu Jen Catholic University, New Taipei City 242, Taiwan

[2] Data Science Center, College of Medicine, Fu Jen Catholic University, New Taipei City 242, Taiwan

[3] School of Medicine, Fu-Jen Catholic University, New Taipei City 242, Taiwan

[4] Division of Nephrology, Department of Internal Medicine, Shin-Kong Wu Ho-Su Memorial Hospital, Taipei, Taiwan

[5] Division of Digital Informatics Management, Department of Digital Medicine, Shin Kong Wu Ho-Su Memorial Hospital, Taiwan

*Corresponding author. E-mail address: chungkuan.wu@gmail.com (Chung-Kuan Wu)

ABSTRACT

Background: This study aims to assess mitral regurgitation (MR) severity's correlation with patients' clinical and cardiac status, along with its association with cardiovascular outcomes and overall mortality in hemodialysis (HD) patients. ***Methods:*** A total of 238 adult chronic HD patients with echocardiography records from October to December 2018 were enrolled in the study and were followed until the end of 2021, transfer, or death. Mitral regurgitation (MR) severity was defined by effective regurgitant orifice area: <0.2 cm² (mild), 0.2–0.4 cm² (moderate), and ≥0.4 cm² (severe). Patients were grouped as none, mild, and moderate-to-severe MR. Association of MR severity with major adverse cardiovascular events (MACEs), cardiovascular, and overall mortality was evaluated, with additional risk factors explored through subgroup analysis. ***Results:*** Among 238 HD patients, 48 had no MR, 157 had mild MR, and 33 had moderate-to-severe MR. Those with moderate-to-severe MR showed more left ventricular (LV) hypertrophy, higher inferior vena cava diameter, and lower LV ejection fraction (LVEF), exhibited lower body weight, triglycerides, platelets, and higher alkaline-phosphatase and peripheral arterial disease prevalence. Compared to no MR, moderate-to-severe MR increased the risk of MACEs, cardiovascular, and

overall mortality (adjusted HRs: 2.18, 4.57, 4.59; 95% CI: 1.02–4.67, 1.40–14.94, 1.60–13.20, respectively). These risks remained significant during follow-up (log-rank $p < 0.05$). For mild MR patients, LVEF <50% significantly increased MACEs risk. ***Conclusion:*** Moderate-to-severe MR increases MACEs, cardiovascular and overall mortality risk in chronic HD patients. An LVEF <50% is a key determinant for MACEs in mild MR patients.

Nonstandard abbreviations and acronyms: AST, aspartate aminotransferase; AVA, arteriovenous access; CAD, coronary artery disease; COPD, chronic obstructive pulmonary disease; CV, cardiovascular; EF, ejection fraction; ESKD, end-stage kidney disease; HD, hemodialysis; iPTH, intact Parathyroid hormone; IVCD, inferior vena cava diameter; IVS, interventricular septum; Kt/V, hemodynamic efficiency; LA, left atrium; LAE, left atrial enlargement; LVEDD, LV end-diastolic diameter; LVPW, LV posterior wall; LV, left ventricle; LVESD, LV end-systolic diameter; LVEF, LV ejection fraction; LVMI, LV mass index; MAC, mitral annular calcification, MACEs, major adverse cardiovascular events; MR, mitral regurgitation; MVP, mitral valve prolapse; PAD, peripheral arterial disease; PISA, proximal isovelocity surface area; RAAS, renin-angiotensin-aldosterone system; RWT, relative wall thickness; SD, standard deviation

Keywords: mitral regurgitation; major adverse cardiovascular outcomes; mortality; hemodialysis

INTRODUCTION

Valvular heart disease (VHD), affecting primarily the aortic and mitral valves, is prevalent among patients with chronic kidney disease (CKD), with prevalence increasing as renal function declines. Therefore, patients with end-stage kidney disease (ESKD), particularly those undergoing hemodialysis (HD), exhibit the highest prevalence [1]. Risk factors for VHD among patients with ESKD include traditional cardiovascular risk factors—such as older age, hypertension, diabetes mellitus, and dyslipidemia—as well as CKD-specific risk factors, including CKD–mineral and bone disorder (CKD-MBD), chronic inflammation, oxidative stress, uremic toxins, altered hemodynamics, and hypoalbuminemia [2-5]. Among ESKD patients with VHD, mitral regurgitation accounts for the highest prevalence, followed by aortic regurgitation, aortic stenosis, and mitral stenosis [2]. Mitral regurgitation (MR) is a common valvular heart disease, affecting about 10% of the total population worldwide [6]. The prevalence of MR in end-stage kidney disease (ESKD) patients on hemodialysis (HD) widely varies from 36.7% to 73.7%, depending on the comorbidities, ESKD etiology, and HD vintage [7]. MR is caused by abnormalities of the cardiac and valvular structures, including papillary muscle or leaflet rupture, mitral annular calcification, and mitral valve prolapse (MVP) [6,8]. The risk factors or diseases associated with MR include older age, male sex, coronary artery disease (CAD), connective tissue disorders, infective endocarditis, congenital heart disease, and hypertension [9,10].

In patients with MR, the backward flow of blood into the left atrium (LA) results in an increase in left atrial pressure, which is transmitted to the left ventricle (LV), potentially increasing the volume or pressure on the LV and eventually resulting in LV remodeling (eccentric or concentric hypertrophy) or dysfunction (heart failure with reduced ejection fraction) [11]. Patients with these cardiac structural abnormalities present with fatigue, dyspnea, palpitations, and symptoms of heart failure [12]. In addition, cardiac structural abnormalities from MR were found to be indicators of poor CV outcomes, which were dependent on the severity of MR [13].

Using echocardiographic data from 78,000 patients, Bansal et al. found significantly lower

five-year survival rates across all degrees of mitral regurgitation (MR) severity in individuals with chronic kidney disease (CKD) compared to those without CKD [14]. These findings are further supported by interventional studies, including transcatheter edge-to-edge repair (M-TEER) trials, which consistently demonstrate poor outcomes among patients with CKD, underscoring the adverse prognostic impact of moderate-to-severe MR in these populations [15–18]. The five-year survival rate of CAD patients was 62% in those without MR compared with 39% in those with MR [19]. Among patients with LV systolic dysfunction, those with moderate-to-severe MR had a three-year mortality rate of 60% compared 21% for those without [20]. In addition, MR patients with atrial fibrillation or heart failure are at a significantly high risk of major adverse cardiovascular events (MACEs) and overall mortality [8,21,22]. The association between MR and CV outcomes among chronic HD patients has not been well studied. This study investigates the correlation between MR, according to severity, on MACE, cardiac mortality, and overall mortality among chronic HD patients.

MATERIALS AND METHODS

Study population and definition of MR severity

This observational cohort study was conducted at a single medical center in Taiwan. We enrolled 241 adult chronic HD patients who were treated at the HD unit of the medical center via functional arteriovenous access and received echocardiography on the mid-week non-dialysis day between October 1, 2018, and December 31, 2018. Exclusion criteria included patients without MR assessment (n = 3). The study ultimately included 238 adult chronic HD patients who had functional AVA with an echocardiography report. Data for this study were accessed and extracted from the institutional database between October 1 and December 31, 2018. The observation period was from the date of echocardiography until the end of 2021 or the time of death, whichever occurred first. The patients were divided into non-, mild-, and moderate-to-severe MR groups on the basis of their echocardiography results (Figure 1). The degree of MR, if present, was graded as none/trivial, mild, moderate, or severe using an integrated approach. Effective regurgitant orifice area by proximal isovelocity surface area was used to quantify MR severity (<0.2 cm2, mild; 0.2–0.4 cm2, moderate; and ≥ 0.40 cm2, severe) [7].

History, Collection, and Laboratory Data

Patients' data were retrospectively collected as part of the study cohort. Given the retrospective nature of the study, laboratory and clinical data were retrieved in accordance with the study's commencement date on October 1, 2018. Data extraction for research purposes was conducted between October 1 and December 31, 2018. Demographic and baseline clinical data for patients undergoing chronic HD were documented at the time of study registration. The data included parameters such as age, sex, weight, HD vintage, comorbid history (including type 2 diabetes mellitus [DM], hypertension, hyperlipidemia, CAD, peripheral arterial disease [PAD], heart failure, chronic obstructive pulmonary disease, malignancy, connective tissue disease, and rheumatic fever), and laboratory results (serum total protein, serum albumin, aspartate aminotransferase, alkaline phosphatase [Alk-P], total bilirubin, serum cholesterol, serum triglycerides, fasting glucose, hemoglobin, serum platelet, iron profile, serum aluminum, serum uric acid, sodium, potassium, ionized calcium, and phosphate levels, along with HD efficiency [Kt/V] and intact parathyroid hormone). Blood samples were collected after a minimum fasting period of eight hours before each HD session, and Kt/V was calculated using the Sargent formula. Patient use of antihypertensive, antidiabetic, antiplatelet, and anticoagulant drugs was also recorded.

Measurement of echocardiographic parameters

The standardized transthoracic echocardiography in the study was performed by a professional cardiologist using M mode or 2D echocardiographic linear measurements. Cardiac chamber quantification and other standard structural parameters such as inferior vena cava diameter (IVCD), interventricular septum (IVS), LA diameter, LV end diastolic diameter (LVEDD), LV end systolic diameter (LVESD), LV posterior wall (LVPW), LV mass index (LVMI), relative wall thickness (RWT), and ejection fraction (EF) were measured according to the recommendations of the American Society of Echocardiography 7. Mitral valve calcification can be detected through echocardiography by visualizing echogenic densities or calcium deposits on the valve leaflets or the mitral annulus.

Outcome measurements

The outcomes in this study included all-cause mortality, CV mortality, and MACE, which is defined as the occurrence of any of the following events: myocardial infarction, coronary revascularization, stroke, or hospitalization for heart failure or death owing to CV etiology.

Statistical analysis

The patients' baseline characteristics were expressed as percentages for categorical data and the mean ± standard deviation for continuous data. Categorical variables were compared using the chi-squared test or Fisher's exact test for numbers lower than 5, while continuous variables were compared using one-way analysis of variance (ANOVA) or the Kruskal–Wallis test, depending on whether the distribution was normal. The incidence of all-cause mortality, CV mortality, and MACE was calculated by computing the number of person-years at risk for each participant from the date of enrollment to the outcome onset, the date of death, or the end of follow-up (December 31st, 2021), whichever came first. Univariate Cox regression analysis was conducted to estimate the crude hazard ratio (cHR) and the 95% confidence interval (CI) for all-cause mortality, CV mortality, and MACE in patients with no, mild, and moderate-to-severe MR. In the multivariate Cox proportional hazards models, confounding variables such as age and sex, with/without all significant variables listed in Table 1, were adjusted to estimate the adjusted hazard ratio (aHR) for outcome events in each of the three groups. The Nelson–Aalen method was used to calculate the cumulative risk of all-cause mortality, CV mortality, and MACEs for the three groups during follow-up; the three groups were compared using the log-rank test. All statistical analyses were performed using SAS version 9.4 with statistical significance set at a two-sided p value < 0.05.

RESULTS

Baseline clinical and echocardiographic characteristics of the study population

Analysis of the baseline and clinical characteristics of the 238-patient cohort revealed the prevalence of the following valvular conditions: MR, 79.8%; aortic regurgitation, 42.4%; aortic stenosis, 11.3%; and mitral stenosis 1.3%. The study population was subsequently divided into three groups based on the severity of MR in echocardiographic findings: no MR (n = 48), mild (n = 157), and moderate-to-severe (n = 33) (Table 1). Patients with moderate-to-severe MR had significantly lower body weight and a higher proportion (30.3%) of PAD compared with the other two groups (p = 0.003, 0.034, respectively). Regarding laboratory test results, the group with moderate-to-severe MR had the highest serum aspartate aminotransferase and Alk-P and the lowest triglyceride and platelet levels of the three groups (all $p < 0.05$, Table 1). The group of patients with no MR had the highest serum potassium level (p = 0.018).

The echocardiographic data presented in Table 2 indicate that patients in the moderate-to-severe MR group had significantly higher values for IVS, LVEDD, LVESD, LVPW, LV mass, LVMI, and IVCD, while patients with no MR had the lowest values (all $p < 0.05$). The moderate-to-severe MR group had the highest proportion of LV hypertrophy, regardless of whether the LV hypertrophy was concentric or eccentric (p = 0.038). Patients with moderate-to-severe MR had the lowest EF values, while those without MR had the highest EF values ($p < 0.001$).

Association of mitral regurgitation with MACEs among chronic HD patients

Cox proportional hazards analysis of outcome events (Table 3) revealed that patients with moderate-to-severe MR had a significantly higher risk of MACE. Adjusted Cox regression analysis showed that this risk was more than two times higher (aHR, 2.18; 95% CI, 1.02–4.67; p = 0.045) than for patients without MR. The cumulative risk of MACE among these patients was also significantly higher than for in the other two groups during follow-up (log rank p = 0.047) (Figure 2A).

Association of mitral regurgitation with cardiovascular and overall mortality among chronic HD patients

Patients with moderate-to-severe MR exhibited significantly higher risk of CV mortality and overall mortality relative to those without MR. In comparison to the no-MR group, the crude and two adjusted HRs for CV mortality in the moderate-severe MR group were 4.94 (95% CI, 1.57–15.5), 4.21 (95% CI, 1.33–13.34), and 4.57 (95% CI, 1.40–14.94), respectively. As for overall mortality, the crude and two adjusted HRs in the moderate-to-severe MR group were 4.99 (95% CI, 1.80–13.86), 4.16 (95% CI, 1.49–11.65), and 4.59 (95% CI, 1.60–13.20), respectively. During the follow-up period, the analysis revealed that patients with moderate-to-severe MR had higher CV ($p < 0.002$) and higher overall mortality (p = 0.006) (Figure 2B and 2C).

Subgroup

Subgroup analysis showed that for mild MR, the HR for MACEs was 1.79 (95% CI, 1.00–3.21) among patients with left atrial enlargement (LAE) compared with those without. Moreover, LVEF ≤ 50% remained a risk for MACEs among patients with mild MR (HR, 2.79; 95% CI, 1.08–7.23) (Figure 3A). Among patients

≥ 65 years of age with mild MR, the presence of LAE and LVEF ≤ 50% posed a higher but not significant risk of CV and overall mortality (Figures 3B, 3C). Among patients with moderate-to-severe MR, age ≥ 65, the presence of LAE, and LVEF ≤ 50% also had a trend toward a higher risk of MACEs, CV, and overall mortality, but differences from those without were insignificant (Figure 3D, 3E, 3F).

DISCUSSION

We observed that chronic HD patients with moderate-to-severe MR had lower body weight, serum triglycerides, and platelet counts, and higher Alk-P and prevalence of PAD than did those with no or milder MR. Moderate-to-severe MR leads to LV hypertrophy, high IVCD, and low LVEF. We found that moderate-to-severe MR is associated with a higher risk and incidence of MACEs, CV mortality, and overall mortality among chronic HD patents. In chronic HD patients with mild MR, the presence of LAE and LVEF ≤ 50% is a risk for MACEs.

Our findings are consistent with several studies demonstrating an inverse relationship between body weight and triglyceride levels with CV disease. The theories of "obesity paradox" and "triglyceride paradox" postulate that the poor nutritional status and lower muscle mass in moderate-to-severe MR leads to more symptoms of heart failure, including dyspnea and fatigue, causing patients to limit their food intake and decrease their physical activity [23]. An association between high serum Alk-P and low muscle mass and malnutrition was also reported in chronic HD patients [24,25]. Low platelet counts observed among patients with moderate-to-severe MR might result from a greater degree of platelet activation in response to their severe hemodynamic abnormalities [26]. The higher prevalence of PAD observed in moderate-to-severe MR patients might also be explained by an increased occurrence of atherosclerosis and low distal artery perfusion caused by more severe MR [27]. The aforementioned findings emphasize the importance of integrating nutritional assessment, sarcopenia screening, and vascular evaluation into the comprehensive care of chronic HD patients with moderate-to-severe MR.

Moderate-to-severe MR patients typically have high IVCD levels, high proportions of LVH and concentric LVH, and low EF. The sympathetic and renin-angiotensin-aldosterone system is activated to maintain adequate stroke volume in the presence of mitral valve regurgitation, leading to increased heart contractility and sodium and water reabsorption. The end results of these physiological changes include high levels of IVCD, LVH, and concentric LVH. Initially, this regulatory system can compensate to achieve adequate cardiac output; however, prolonged stretching of the LV chamber with time as the severity of the regurgitation increases results in deterioration of LV contractile function, leading to low EF. These findings highlight the critical role of cardiac monitoring in chronic HD patients with moderate-to-severe MR. Accordingly, echocardiographic surveillance—including assessment of IVCD, left ventricular geometry, and ejection fraction—can facilitate early detection of cardiac decompensation, optimize fluid and medical management, and support timely referral for valve intervention, potentially improving outcomes in this high-risk population.

This present study indicates that moderate-to-severe MR is a risk factor for MACE and CV mortality among chronic HD patients. Accordingly, dysregulation of the compensation system might lead to a decline in LV function that subsequently causes the cardiac output to decrease and the LA to change morphologically. Therefore, the incidence of heart failure, atrial fibrillation [28], and potentially coronary hypoperfusion, a well-known risk factor for stroke, increases with MR severity. Thus, the incidence of CV mortality increases with MR severity because of the increased risk of fatal arrythmia, heart failure, and myocardial infarction.

Moderate-to-severe MR was also found to be a risk factor for all-cause mortality in this study. In addition to the high incidence of CV and cerebrovascular mortality among patients with moderate-to-severe MR, other causes of mortality might increase in this population. For example, moderate-to-severe MR leads to pulmonary hypertension, subsequent interstitial pulmonary fibrosis. and pneumonia, thereby increasing the mortality rate in this population [29]. Accordingly, in chronic HD patients with moderate-to-severe MR, comprehensive and regular evaluation of cardiac function, arrhythmia, coronary artery disease, and pulmonary status is essential for early identification and aggressive management of these complications to reduce the risk of MACE, CV and all-cause mortality.

Subgroup analysis showed that mild MR patients with LAE and LVEF ≤ 50% had a higher risk of MACE, CV, and overall mortality. This finding is consistent with other studies reporting that LAE is independently associated with all-cause mortality because LAE increases the risk of atrial fibrillation, stroke, and heart failure [30]. However, no study has determined why LAE is more significant in patients with mild MR than

in those without or with moderate-to-severe MR. We postulate that patients with mild MR have a low incidence of MACEs mainly due to their sufficient tolerance to volume buildup. However, if MR is complicated with LAE, then structural changes may disturb the LV compensation mechanisms either via conduction or hemodynamic disturbances. This effect may not be as significant as in moderate-to-severe MR patients because their compensatory mechanisms are already compromised. One other possible explanation is that moderate-to-severe MR patients may have another more dominant factor at play that influences MACE, CV mortality, and overall mortality. In MR patients with LVEF, the MR compensatory mechanics allow for more LV emptying to maintain adequate forward blood flow, causing EF to increase [31]. EF may even rise in severe MR patients with normal LV function. Therefore, a decrease in LVEF at an earlier stage, as in mild MR patients where volume buildup is less, may reflect very poor contractile dysfunction that could explain the worse outcomes among these patients. Although chronic HD patients with mild MR had better MACEs, CV and all-cause mortality than those with moderate-to-severe MR, we still need to carefully understand whether there is LAE and poor EF in chronic HD patients with mild MR based on the study results. LAE is a well-established marker of chronic left atrial pressure/volume overload and a predictor of atrial fibrillation, stroke, and heart failure 4. An LVEF ≤50% can indicate early LV systolic dysfunction, particularly ominous with limited cardiac reserve 32. Therefore, cardiac morphology and function should still be measured and followed in chronic HD patients with mild MR.

This study has several limitations. First, the cohort sample size was relatively small, which may limit statistical power. Second, the data were collected from a single urban medical center, and nearly all enrolled patients were of Han Chinese ethnicity; thus, the findings may potentially limited generalizability to broader or more diverse populations. Third, the etiology of MR could not be determined within this dataset. Fourth, important clinical variables such as fluid management and medication use during follow-up – both of which might affect the outcomes – were not accounted for.

CONCLUSIONS

In chronic HD patients, moderate-to-severe MR is a risk factor for MACEs, CV mortality, and overall mortality. Among HD patients with mild MR, LVEF < 50% is a determining factor for the occurrence of MACEs.

DECLARATIONS

Declaration of competing interest

All authors have no conflicts of interest to declare

Institutional Review Board Statement: This study was performed in accordance with the principles of the Declaration of Helsinki. The need for written informed consent was waived by the Shin-Kong Wu Ho-Su Memorial Hospital ethics committee (IRB number: 20220901R) due to retrospective nature of the study. The authors declare that they have no conflict of interest.

Funding: This research was supported by grants from the Shin Kong Wu Ho-Su Memorial Hospital Research Foundation with College of Medicine, Fu-Jen Catholic University. The grant number was 112-SKH-FJU-04. We sincerely appreciate their support and the funding source played no role in the study design, data collection, analysis, or interpretation of results.

CRediT authorship contribution statement

Wan-Lun Hsu Conceptualization – Methodology – Validation – Writing original draft – Review & editing. **Yukiko Ono** Formal analysis – Methodology – Validation. **Zhi-Yi Lee** Validation. **Shiou-Cheng Hu** Validation – Writing original draft – Review & editing. Noi Yar Methodology – Validation. **Ya Ker Huang** Data curation – Validation. **Chung-Kuan Wu** Conceptualization – Data curation – Methodology – Supervision –Validation – Funding acquisition – Writing original draft –Review & editing.

Data Availability Statement

The data underlying this article will be shared on reasonable request to the corresponding author.

Supplementary materials

Supplementary material associated with this article can be found in the online version at https://doi.org/...

REFERENCES

1. Adam EL. Progression of valvular heart disease in dialysis patients: how to stop it?. J Bras Nefrol. 2024;46(2):e2024E005. doi:10.1590/2175-8239-JBN-2024-E005en
2. Marwick TH, Amann K, Bangalore S, et al. Chronic kidney disease and valvular heart disease: conclusions from a Kidney Disease: Improving Global Outcomes (KDIGO) Controversies Conference.

Kidney Int. 2019;96(4):836-849. doi:10.1016/j.kint.2019.06.025

3. Bover J, Aguilar A, Arana C, et al. Clinical approach to vascular calcification in patients with non-dialysis dependent chronic kidney disease: mineral-bone disorder-related aspects. Front Med (Lausanne). 2021;8:642718. doi:10.3389/fmed.2021.642718
4. Zhang J, Pang Q, Wang S, Wu L, Zhang A. Associated factors of cardiac valve calcification and its prognostic effects among patients with chronic kidney disease: a systematic review and meta-analysis. Front Cardiovasc Med. 2023;10:1120634. doi:10.3389/fcvm.2023.1120634
5. Jankowski J, Floege J, Fliser D, Böhm M, Marx N. Cardiovascular disease in chronic kidney disease: pathophysiological insights and therapeutic options. Circulation. 2021;143(11):1157-1172. doi:10.1161/CIRCULATIONAHA.120.050686
6. Wu S, Chai A, Arimie S, et al. Incidence and treatment of severe primary mitral regurgitation in contemporary clinical practice. Cardiovasc Revasc Med. 2018;19(8):960-963. doi: 10.1016/j.carrev.2018.07.021
7. Ahmed MI, McGiffin DC, O'Rourke RA, et al. Mitral regurgitation. Curr Probl Cardiol. 2009;34(3):93-136. doi:10.1016/j.cpcardiol.2008.11.002
8. Kim M, Kim D, Lee J, et al. Mitral and aortic regurgitation in patients undergoing kidney transplantation: the natural course and factors associated with progression. Front Cardiovasc Med. 2022;9:809707. doi:10.3389/fcvm.2022.809707
9. Enriquez-Sarano M, Avierinos JF, Messika-Zeitoun D, et al. Quantitative determinants of the outcome of asymptomatic mitral regurgitation. N Engl J Med. 2005;352(9):875-883. doi:10.1056/NEJMoa041451
10. Rahimi K, Mohseni H, Otto CM, et al. Elevated blood pressure and risk of mitral regurgitation: A longitudinal cohort study of 5.5 million United Kingdom adults. PLoS Med. 2017;14(10):e1002404. doi:10.1371/journal.pmed.1002404
11. Apostolidou E, Maslow AD, Poppas A. Primary mitral valve regurgitation: Update and review. Glob Cardiol Sci Pract. 2017;2017(1):e201703. doi:10.21542/gcsp.2017.3
12. Nishimura RA, Otto CM, Bonow RO, et al. 2014 AHA/ACC Guideline for the management of patients with valvular heart disease: executive summary: a report of the american college of cardiology/american heart association task force on practice guidelines. Circulation. 2014;129(23):2440-2492. doi:10.1161/CIR.0000000000000029
13. Kim DY, Seo J, Cho I, et al. Prognostic implication of mitral valve disease and its progression in east asian patients with hypertrophic cardiomyopathy. J Am Heart Assoc. 2023;12(3):e024792. doi:10.1161/JAHA.121.024792
14. Samad Z, Sivak JA, Phelan M, Schulte PJ, Patel U, Velazquez EJ. Prevalence and outcomes of left-sided valvular heart disease associated with chronic kidney disease. J Am Heart Assoc. 2017;6(10):e006044. doi:10.1161/JAHA.117.006044
15. Tanaka K, Yamaguchi J, Yoshikawa M, et al. Effect of renal impairment on clinical outcomes after mitral valve transcatheter edge-to-edge repair. JACC Asia. 2025;5(2):273-282. doi:10.1016/j.jacasi.2024.10.025
16. Ohno Y, Attizzani GF, Capodanno D, et al. Impact of chronic kidney disease on outcomes after percutaneous mitral valve repair with the MitraClip system: insights from the GRASP registry. EuroIntervention. 2016;11(14):e1649-e1657. doi:10.4244/EIJV11I14A316
17. Shah B, Villablanca PA, Vemulapalli S, et al. Outcomes after transcatheter mitral valve repair in patients with renal disease. Circ Cardiovasc Interv. 2019;12(2):e007552. doi:10.1161/CIRCINTERVENTIONS.118.007552
18. Sisinni A, Munafò A, Pivato CA, et al. Effect of chronic kidney disease on 5-year outcome in patients with heart failure and secondary mitral regurgitation undergoing percutaneous MitraClip insertion. Am J Cardiol. 2022;171:105-114. doi:10.1016/j.amjcard.2022.01.048
19. Grigioni F, Enriquez-Sarano M, Zehr K KJ, et al. Ischemic mitral regurgitation: long-term outcome and prognostic implications with quantitative Doppler assessment. Circulation. 2001;103(13):1759-1764. doi:10.1161/01.cir.103.13.1759

20. Koelling TM, Aaronson KD, Cody R J, et al. Prognostic significance of mitral regurgitation and tricuspid regurgitation in patients with left ventricular systolic dysfunction. Am Heart J. 2002;144(3):524-529. doi:10.1067/mhj.2002.123575
21. Düren DR, Becker AE, Dunning AJ. Long-term follow-up of idiopathic mitral valve prolapse in 300 patients: a prospective study. J Am Coll Cardiol. 1988;11(1):42-47. doi:10.1016/0735-1097(88)90164-7
22. Tribouilloy CM, Enriquez-Sarano M, Schaff HV, et al. Impact of preoperative symptoms on survival after surgical correction of organic mitral regurgitation: rationale for optimizing surgical indications. Circulation. 1999;99(3):400-405. doi:10.1161/01.cir.99.3.400
23. Xia TL, Li YM, Huang FY, et al. The triglyceride paradox in the mortality of coronary artery disease. Lipids Health Dis. 2019;18(1):21. doi:10.1186/s12944-019-0972-0
24. Tutor AW, Lavie CJ, Kachur S, et al. Updates on obesity and the obesity paradox in cardiovascular diseases. Prog Cardiovasc Dis. 2023;78:2-10. doi:10.1016/j.pcad.2022.11.013
25. Velasquez-Mao AJ, Velasquez MA, Hui Z, et al. Hemodialysis exacerbates proteolytic imbalance and pro-fibrotic platelet dysfunction. Sci Rep. 2021;11(1):11764. doi:10.1038/s41598-021-91416-8
26. Tse HF, Lau CP, Cheng G. Relation between mitral regurgitation and platelet activation. J Am Coll Cardiol. 1997;30(7):1813-1818. doi:10.1016/s0735-1097(97)00380-x
27. Nakaya H, Yokoyama N, Watanabe Y, et al. Prevalence and predictors of atherosclerotic peripheral arterial obstructive disease in severe heart valve diseases. Int Heart J. 2020;61(4):727-733. doi:10.1536/ihj.20-009
28. Delgado V, Bax JJ. Atrial functional mitral regurgitation: from mitral annulus dilatation to insufficient leaflet remodeling. Circ Cardiovasc Imaging. 2017;10(3):e006239. doi:10.1161/CIRCIMAGING.117.006239
29. Ratwatte S, Strange G, Playford D, et al. Prevalence of pulmonary hypertension in mitral regurgitation and its influence on outcomes. Open Heart. 2023;10(1):e002268. doi:10.1136/openhrt-2023-002268
30. Barbieri A, Bursi F, Grigioni F, et al. Prognostic and therapeutic implications of pulmonary hypertension complicating degenerative mitral regurgitation due to flail leaflet: a multicenter long-term international study. Eur Heart J. 2011;32(6):751-759). doi:10.1093/eurheartj/ehq294
31. Detaint D, Messika-Zeitoun D, Avierinos JF, et al. B-type natriuretic peptide in organic mitral regurgitation: determinants and impact on outcome. Circulation. 2005;111(18):2391-2397. doi:10.1161/01.CIR.0000164269.80908
32. Yamada S, Ishii H, Takahashi H, et al. Prognostic value of reduced left ventricular ejection fraction at start of hemodialysis therapy on cardiovascular and all-cause mortality in end-stage renal disease patients. Clin J Am Soc Nephrol. 2010;5(10):1793-1798. doi:10.2215/CJN.00050110

FIGURE AND FIGURE LEGENDS

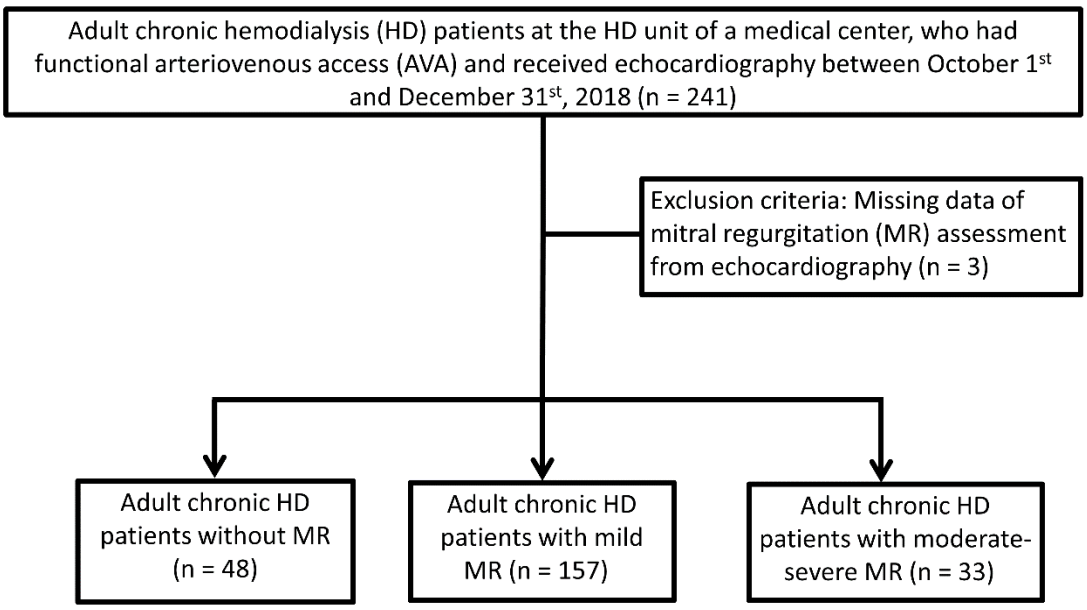

Figure 1. Flowchart for enrollment of chronic HD patients into the study cohort.

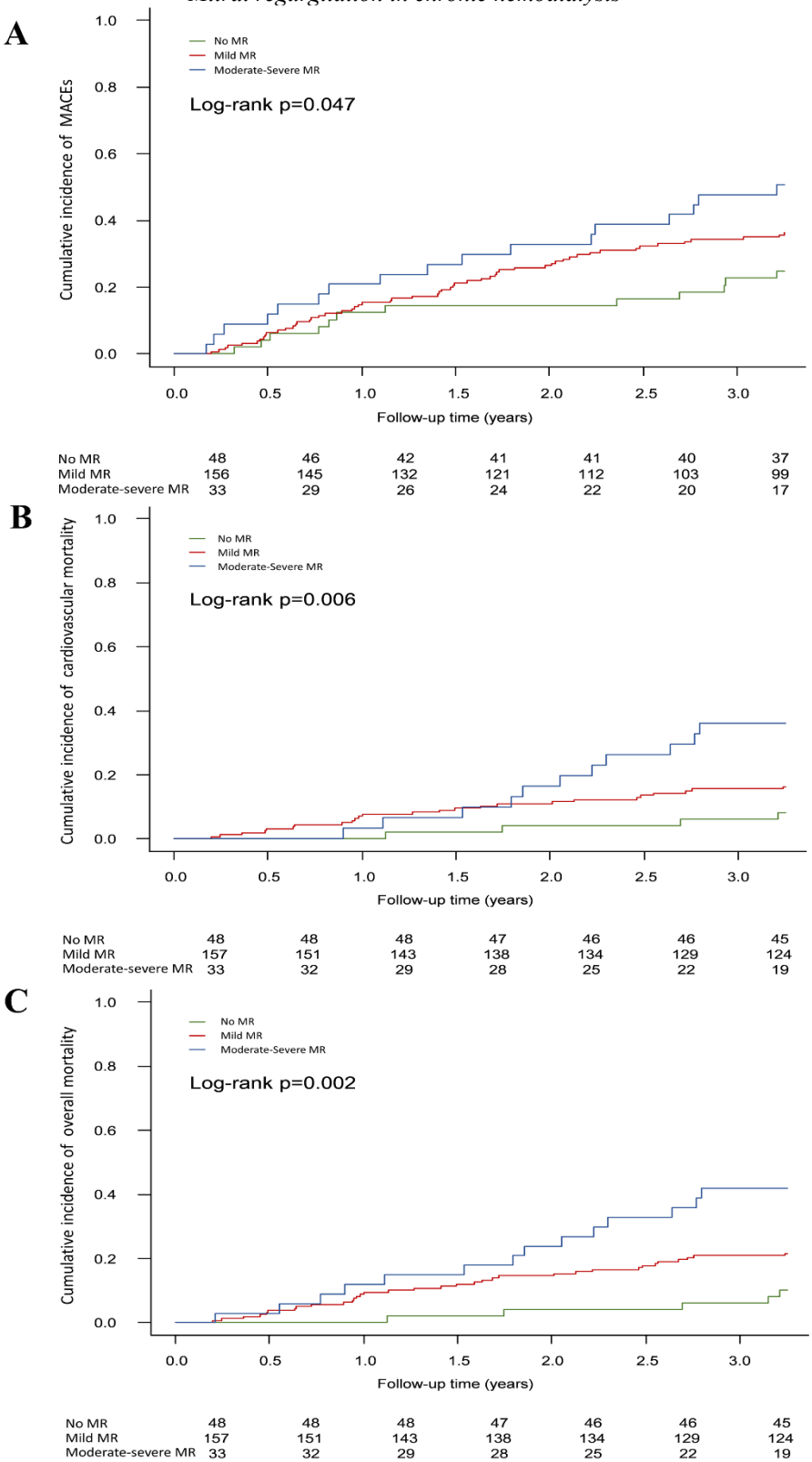

Figure 2. Kaplan–Meier curves for the cumulative incidence of MACE (A), cardiovascular survival (B), and overall survival (C) among chronic HD patients according to MR severity during three years of follow-up.

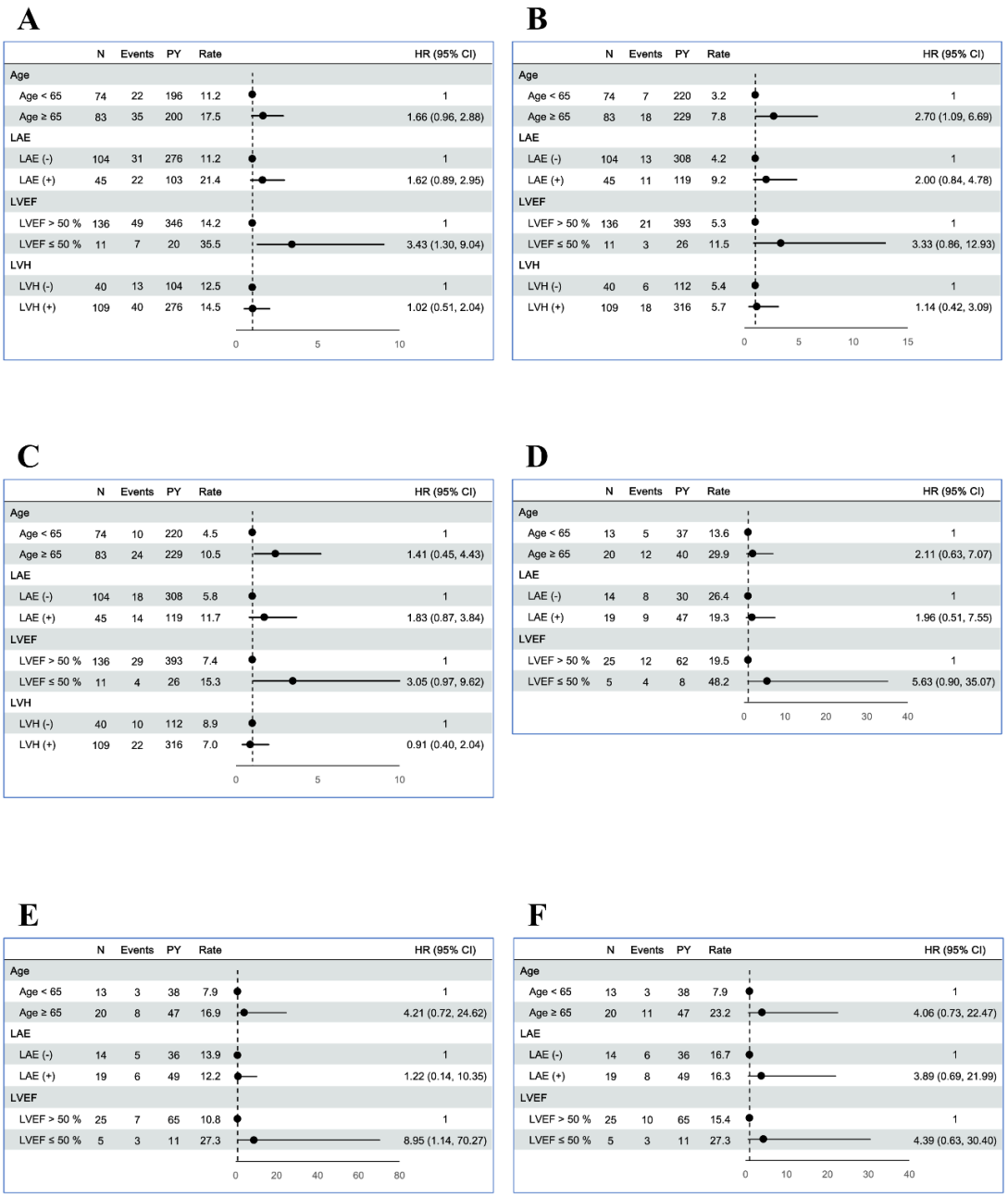

Figure 3. Forest plot for subgroup risk analysis of mild MR for MACEs (A), cardiovascular mortality (B), and overall mortality (C) and of moderate-to-severe MR for MACEs (D), cardiovascular mortality (E), and overall mortality (F). HRs are adjusted for age, sex, PAD, platelet, potassium, insulin, and insulin analogs.

TABLES

Table1. Baseline characteristics of chronic HD patients according to severity of MR

	MR (–)	Mild MR	Moderate/severe MR	*p*
Number of patients	48	157	33	---
Age (years)	63.4±12.4	65.1±12.0	67.2±14.5	0.407*
Sex, female (%)	25 (52.1)	69 (43.9)	15 (45.5)	0.612†
Weight (kg)	60.8 (52.5,74.5)	58.8 (51.0,69.0)	51.0 (43.5,61.2)	0.003§
Hemodialysis vintage (years)	6.3 (2.0,11.2)	5.7 (2.8,12.0)	5.2 (2.6,9.6)	0.771§
Comorbidities (%)				
Type 2 DM	17 (35.4)	73 (46.5)	13 (39.4)	0.355†
Hypertension	37 (77.1)	123 (78.3)	26 (78.8)	0.979†
Hyperlipidemia	24 (50.0)	85 (54.1)	14 (42.4)	0.457†
CAD	15 (31.3)	66 (42.0)	14 (42.4)	0.390†
PAD	5 (10.4)	42 (26.8)	10 (30.3)	0.044†
Heart failure	9 (18.8)	30 (19.1)	8 (24.2)	0.782†
COPD	2 (4.2)	16 (10.2)	6 (18.2)	0.127‡
Malignancy	5 (10.4)	19 (12.1)	2 (6.1)	0.741‡
Connective tissue disease	0 (0.0)	3 (1.9)	0 (0.0)	1.000‡
Rheumatic fever	0 (0.0)	2 (1.3)	0 (0.0)	1.000‡
Laboratory data				
Albumin (gm/dL)	4.0 (3.7,4.1)	3.9 (3.7,4.1)	3.9 (3.6,4.0)	0.168§
A.S.T. (IU/L)	15.5 (12.0,18.0)	15.0 (12.0,19.0)	17.0 (13.0,25.0)	0.154§
Alkaline-P (IU/L)	61.5 (50.5,75.5)	65.0 (52.0,83.0)	76.0 (60.0,112.0)	0.013§
Cholesterol (mg/dL)	157.5 (142.0,186.5)	151.0 (128.0,176.0)	155.0 (131.0,182.0)	0.272§
Triglyceride (mg/dL)	117.0 (95.5,177.0)	108.0 (81.0,168.0)	70.0 (51.0,105.0)	<0.001§
Fasting glucose	89.0 (82.5,114.0)	94.0 (85.0,121.0)	95.0 (84.0,124.0)	0.610§

(mg/dL)				
Hemoglobin (g/dL)	10.3 (9.6,11.1)	10.3 (9.6,11.1)	9.9 (9.4,10.4)	0.143§
Platelet (×1000/μL)	212.8±58.5	188.3±55.1	173.7±54.4	0.005*
Ferritin (ng/mL)	581.1 (429.0,731.8)	544.7 (437.1,688.3)	584.1 (446.5,668.2)	0.792§
Al (ng/mL)	5.9 (4.6,8.3)	6.0 (4.6,7.6)	5.6 (4.0,9.4)	0.841§
Uric acid (mg/dL)	6.8 (5.7,7.4)	6.3 (5.4,7.2)	6.3 (5.8,7.0)	0.535§
Na (meq/L)	138.0 (136.5,140.0)	138.0 (136.0,140.0)	138.0 (136.0,139.0)	0.800§
K (meq/L)	4.9 (4.4,5.3)	4.5 (4.2,5.0)	4.7 (4.2,5.1)	0.017§
iCa (mg/dL)	4.6±0.5	4.6±0.5	4.6±0.5	0.921*
P (mg/dL)	5.2 (4.3,5.9)	4.9 (3.9,5.7)	5.2 (4.5,6.3)	0.300§
Kt/V (Gotch)	1.4 (1.3,1.5)	1.4 (1.3,1.5)	1.4 (1.3,1.5)	0.813§
PTH (pg/mL)	253.3 (133.3,436.9)	183.7 (81.7,346.3)	266.5 (129.1,374.4)	0.033§
Medication use (%)				
An-ti-hypertensive drugs				
ACEI/ARB	25 (52.1)	83 (52.9)	20 (60.6)	0.695†
Beta-blockers	19 (39.6)	83 (52.9)	21 (63.4)	0.091†
Calcium antag-onists	29 (60.4)	88 (56.1)	25 (75.8)	0.110†
Calcium-based PB	33 (68.8)	91 (56.0)	18 (54.6)	0.334†
Non-calcium based PB	11 (22.9)	30 (19.1)	9 (27.3)	0.541†
Calcitriol	25 (52.1)	64 (40.8)	13 (39.4)	0.348†
Statins	18 (37.5)	54 (34.4)	11 (33.3)	0.907†
OAD	16 (33.3)	47 (29.9)	7 (21.2)	0.486†
Insulin and an-alogs	3 (6.3)	34 (21.7)	4 (12.1)	0.001†
Antiplatelets	15 (31.3)	72 (45.9)	14 (42.4)	0.201†

Anticoagulants	0 (0.0)	10 (6.4)	0 (0.0)	0.085‡

Data are expressed as n (%) for categorical variables and mean ± standard deviation or median (lower quartile Q1–upper quartile Q3) for continuous variables. DM, diabetes mellitus; PAD, peripheral arterial disease; COPD, chronic obstructive pulmonary disease; AST, aspartate aminotransferase; TSAT, transferrin saturation; Al, aluminum; PTH, parathyroid hormone; ACEI/ARB, angiotensin-converting enzyme inhibitor/angiotensin II receptor blocker; OAD, oral antidiabetic medications; PB, phosphate binders. *One-way ANOVA test §Kruskal Wallis test †Chi-square test ‡Fisher's exact test

Table2. Echocardiographic findings of chronic HD patients according to severity of MR

	MR (–)	**Mild MR**	**Moderate-to-severe MR**	***p***
Aortic root (mm, range)	32.00 (29.50,36.00)	31.00 (29.00,35.00)	32.00 (29.00,34.00)	0.402§
IVS (mm)	11.00 (11.00,13.00)	11.00 (10.00,13.00)	13.00 (12.00,15.00)	0.001§
LA diameter (mm)	41.00 (39.00,45.00)	42.00 (37.00,48.00)	45.00 (41.00,50.00)	0.053§
LVEDD (mm)	47.94±7.07	49.38±7.22	52.26±7.94	0.033*
LVESD (mm)	28.50 (24.00,32.00)	30.00 (26.00,35.00)	37.00 (28.70,39.00)	<0.001§
LVPW (mm)	11.00 (9.00,12.00)	11.00 (9.22,12.00)	11.10 (10.00,13.00)	0.072§
LV mass (g)	213.06 (163.77,252.44)	211.14 (166.87,259.71)	260.53 (222.67,320.08)	0.001§
LVMI§	129.91 (104.55,153.46)	128.41 (106.53,151.16)	166.75 (153.87,212.11)	<0.001§
RWT (mm)	0.45 (0.37,0.54)	0.43 (0.37,0.49)	0.43 (0.38,0.48)	0.757§
IVC diameter (mm)	14.35±3.78	14.77±4.18	17.59±5.04	0.001*
EF (%)	72.00 (67.00,77.50)	69.00 (62.00,76.00)	63.00 (54.00,66.00)	<0.001§
MVC	15 (31.3)	70 (44.6)	13 (39.4)	0.253†
LVH	34 (70.8)	109 (69.4)	31 (93.9)	0.026†
Concentric	19 (39.6)	55 (35.0)	17 (51.5)	0.034†
Eccentric	15 (31.3)	54 (34.4)	14 (42.4)	0.571†
MVP	0 (0.0)	3 (1.9)	2 (6.1)	0.198‡
Leaflet perforation	1 (2.1)	1 (0.6)	1 (3.0)	0.268‡
Mechanical valve	0 (0.0)	4 (2.5)	0 (0.0)	0.767‡

Data are expressed as n (%) for categorical variables and mean ± standard deviation or median (lower quartile Q1–upper quartile Q3) for continuous variables for continuous data. IVS, interventricular septum; LA, left atrium; LVEDD, LV end-diastolic diameter; LVESD, LV end-systolic diameter; LVPW, LV posterior wall; LV, left ventricle; LVMI, LV mass index; IVC, inferior vena cava; EF, ejection fraction; MVC, mitral valve calcification. *One-way ANOVA §Kruskal Wallis †Chi-square test ‡Fisher's exact test

Table3. Cox proportional hazards analysis of major adverse cardiovascular events, cardiovascular mortality, and overall mortality among chronic HD patients

	N	Events	PY	Rate	Crude	Model 1*	Model 2*
					HR (95% CI)	HR (95% CI)	HR (95% CI)
MACEs							
MR (-)	48	12	136	8.8	1.00	1.00	1.00
Mild MR	157	57	396	14.4	1.59 (0.85–2.97)	1.50 (0.80–2.80)	1.32 (0.69–2.53)
Moderate-to-severe MR	33	17	17	22.1	2.48 (1.18–5.20)	2.23 (1.06–4.68)	2.18 (1.02–4.67)
CV mortality							
MR (-)	48	4	152	2.6	1.00	1.00	1.00
Mild MR	157	25	449	5.6	2.13 (0.74–6.11)	1.95 (0.68–5.61)	1.71 (0.58–5.07)
Moderate-to-severe MR	33	11	85	12.9	4.94 (1.57–15.5)	4.21 (1.33–13.34)	4.57 (1.40–14.94)
Mortality							
MR (-)	48	5	152	3.3	1.00	1.00	1.00
Mild MR	157	34	449	7.6	2.31 (0.90–5.90)	2.12 (0.83–5.41)	1.82 (0.70–4.78)
Moderate-to-severe MR	33	14	85	16.5	4.99(1.80,13.86)	4.16 (1.49–11.65)	4.59 (1.60–13.20)

PY: person-years, Rate: incidence rate per 100 person-years. Model 1: adjusted for age and sex; Model 2: adjusted for age, sex, PAD, platelet count, potassium, and insulin and analogs.

Moderate to severe mitral regurgitation affects major adverse cardiovascular outcomes and mortality among chronic hemodialysis patients

中重度二尖瓣逆流對慢性血液透析患者重大不良心血管事件及死亡率的影響

徐婉倫[1,2]　小野由紀子[2]　李知誼[3]　胡修誠[3]　Noi Yar[4]　黃雅哥[4]

吳重寬[3,4,5*]

中文摘要

背景：本研究旨在評估二尖瓣逆流（mitral regurgitation, MR）嚴重程度與慢性血液透析（hemodialysis, HD）患者之臨床與心臟狀況的相關性，以及其與心血管預後及整體死亡率之關聯。**方法：**本研究共納入 2018 年 10 月至 12 月期間接受心臟超音波檢查的 238 名成年慢性 HD 患者，並追蹤至 2021 年底、轉院或死亡。依據 MR 嚴重程度，將患者分為無 MR、輕度 MR 及中重度 MR 三組。進一步分析 MR 嚴重程度與重大不良心血管事件（major adverse cardiovascular events, MACEs）、心血管死亡率及整體死亡率之關聯，並進行亞組分析以辨識其他危險因子。**結果：**238 名 HD 患者中，48 人無 MR、157 人輕度 MR、33 人中重度 MR。中重度 MR 顯著與左心室肥厚、下腔靜脈徑擴大及左心室射出分率（left ventricular ejection fraction, LVEF）降低有關，此外，此群體亦表現出體重較低、三酸甘油脂與血小板數較低、鹼性磷酸酶較高，以及較高的周邊動脈疾病盛行率。與無 MR 者相比，中重度 MR 患者在調整臨床變項後，MACEs、心血管及整體死亡風險顯著增加（調整後風險比[aHR]分別為 2.18、4.57、4.59；95%信賴區間為 1.02–4.67、1.40 – 14.94、1.60 – 13.20）。追蹤期間內，中重度 MR 在統計上仍為上述預後的重要風險因子（log-rank 檢定，$p < 0.05$）。在輕度 MR 患者中，LVEF 低於 50%者之 MACEs 風險顯著升高。**結論：**中重度 MR 顯著增加慢性 HD 患者發生 MACEs、心血管死亡及整體死亡之風險；而在輕度 MR 患者中，LVEF <50% 為 MACEs 的重要預測因子。

關鍵字：二尖瓣逆流、重大不良心血管事件、死亡率、血液透析

[1] 輔仁大學醫學院醫療健康產業大數據分析碩士學位學程

[2] 輔仁大學醫學院數據科學中心

[3] 輔仁大學醫學院醫學系

[4] 台北市新光吳火獅紀念醫院內科部腎臟科

[5] 台北市新光吳火獅紀念醫院數位醫學部數位資訊科

[*]通訊作者：吳重寬　電子信箱 chungkuan.wu@gmail.com

Submitted June 09, 2025.
Final version accepted June 24, 2025.

Cite as: Yao-Jen Chang, Tsung-Ming Chang, Ji-Fan Lin, Ju-Fang Liu, Chi-Jen Chang Multi-Dataset Transcriptomic Analysis Uncovers Loricrin as a Key Suppressor of Melanoma Metastasis
Fu-Jen Journal of Medicine 23(3): 18-32, 2025.
DOI: 10.53106/181020932025092303002

Original Research Article

Multi-Dataset Transcriptomic Analysis Uncovers Loricrin as a Key Suppressor of Melanoma Metastasis

Yao-Jen Chang[1], Tsung-Ming Chang[2], Ji-Fan Lin[3], Ju-Fang Liu[3, 4], Chi-Jen Chang[5, 6*]

[1] Division of Plastic Surgery, Shin Kong Wu Ho-Su Memorial Hospital, Taipei 111045, Taiwan
[2] School of Dental Technology, College of Oral Medicine, Taipei Medical University, Taipei 11031, Taiwan.
[3] Translational Medicine Center, Shin Kong Wu Ho-Su Memorial Hospital, Taipei 111045, Taiwan.
[4] School of Oral Hygiene, College of Oral Medicine, Taipei Medical University, Taipei 11031, Taiwan.
[5] School of Medicine, Fu Jen Catholic University, New Taipei City 24205, Taiwan.
[6] Division of Pediatric Surgery, Shin Kong Wu Ho-Su Memorial Hospital, Taipei 111045, Taiwan.
*Corresponding author. E-mail address: m002008@ms.skh.org.tw (Chi-Jen Chang)

ABSTRACT

Background: Melanoma is a highly aggressive skin cancer with poor prognosis once metastasis occurs. Identifying metastasis-suppressive biomarkers is crucial for improving clinical outcomes. ***Materials and methods:*** We integrated three GEO datasets (GSE65904, GSE59455, GSE8401) to identify differentially expressed genes (DEGs) between metastatic and primary melanoma tissues. GO/KEGG enrichment, PPI network construction, and hub gene analysis were performed using STRING, Cytoscape (MCODE, CytoHubba), and Venn analysis. Clinical significance was validated via GEPIA and OSdream platforms. ***Results:*** We identified 37 overlapping DEGs enriched in keratinocyte differentiation and epithelial barrier functions. loricrin (LOR), Keratin 6B (KRT6B), and filaggrin (FLG) were consistently downregulated in melanoma and identified as hub genes. Among them, LOR expression correlated with longer metastasis-free survival ($p = 0.0466$) and was negatively associated with ADAM12, ITGA4, and CDK1 expression in melanoma. These results suggest that LOR may suppress melanoma metastasis. ***Conclusion:*** LOR is a potential biomarker for predicting melanoma metastasis and progression, highlighting its value for prognosis and therapeutic targeting.

Keywords: melanoma, metastasis, loricrin (LOR), bioinformatics, differentially expressed genes (DEGs)

INTRODUCTION

Melanoma is a highly aggressive form of skin cancer originating from melanocytes and accounts for the majority of skin cancer–related deaths despite representing less than 5% of all cutaneous malignancies [1]. Its incidence has steadily increased worldwide over the past few decades, particularly among fair-skinned populations, posing a growing public health concern [2]. While early-stage melanomas are often curable by surgical excision, advanced or metastatic cases are associated with poor prognosis, with a median survival of approximately 9–12 months and a 5-year survival rate below 25% [1, 2].

Current treatment strategies for advanced melanoma include immune checkpoint inhibitors (e.g., anti-PD-1, anti-CTLA-4 antibodies) and BRAF/MEK-targeted therapies, which have significantly improved overall survival in subsets of patients [1-3]. However, a substantial proportion of patients develop resistance or fail to respond, underscoring the need for novel biomarkers to predict disease progression and identify new therapeutic targets [4]. Among promising biomarkers, recent studies have highlighted ADAM12, ITGA4, and CDK1 for their pivotal roles in melanoma progression. ADAM12, a member of the metalloproteinase family, contributes to tumor cell invasion and metastasis by remodeling the extracellular matrix and enhancing cellular migratory capacities [5]. Similarly, ITGA4 (integrin alpha-4) is involved in mediating cell adhesion and migration, critical for the dissemination of gastric cancer [6]. Additionally, cyclin-dependent kinase 1 (CDK1), a key regulator of cell cycle progression, is frequently upregulated in melanoma, promoting rapid tumor proliferation and resistance to apoptosis [7]. High CDK1 activity has been associated with aggressive tumor behavior and reduced patient survival rates, underscoring its potential as both a prognostic biomarker and therapeutic target in melanoma management [8]. Since distant metastasis is the major driver of melanoma lethality, understanding the molecular mechanisms underlying metastatic spread and discovering robust predictive biomarkers are critical priorities in melanoma research and precision oncology.

Metastasis is a complex, multistep process involving local invasion, epithelial-to-mesenchymal transition (EMT), cytoskeletal remodeling, immune evasion, intravasation, and colonization of distant organs [2, 4]. Melanoma is particularly prone to early systemic dissemination, including to the lungs, liver, brain, and bone [9]. Traditional histopathological parameters, such as Breslow thickness and ulceration status, are insufficient to capture the molecular diversity of metastatic potential across patients [3]. To address this, transcriptomic analyses using high-throughput platforms (e.g., GEO and TCGA) combined with bioinformatics pipelines—such as GO/KEGG enrichment, protein–protein interaction (PPI) network analysis, and hub gene identification algorithms (e.g., MCODE, CytoHubba)—have emerged as powerful tools to uncover differentially expressed genes (DEGs) involved in metastasis [2, 10].

Loricrin (LOR) is a major component of the cornified envelope and plays a central role in terminal keratinocyte differentiation, epithelial barrier formation, and resistance to oxidative stress [11, 12]. It is abundantly expressed in the suprabasal layers of stratified squamous epithelium and has been implicated in barrier-related skin disorders such as ichthyosis, psoriasis, and atopic dermatitis [13, 14]. In cancer, altered LOR expression has been observed in squamous cell carcinomas of the skin, esophagus, and cervix, with roles in cell adhesion, cornification, and epithelial integrity [10, 15]. Recent studies suggest that downregulation of peritumoral LOR is associated with poor prognosis and increased metastasis risk in melanoma, especially when coupled with loss of AMBRA1 expression in the epidermis overlying tumors [16-18]. However, the precise biological role of LOR in melanoma progression and its mechanistic contribution to metastasis remain poorly understood.

In this study, we investigated metastasis-associated gene signatures in melanoma by integrating multiple GEO datasets comparing metastatic and non-metastatic melanoma tissues. Through differential expression analysis, Venn diagram intersection, and functional enrichment, we identified 37 overlapping DEGs associated with keratinocyte differentiation, epithelial barrier regulation, and cytoskeletal remodeling. PPI network construction and hub gene analysis revealed LOR, KRT6B, and FLG as central nodes. Notably, LOR was significantly downregulated in melanoma tissues and demonstrated prognostic value in survival analyses using TCGA and OSdream platforms. Additionally, LOR expression negatively correlated with several metastasis-related DEGs in the GEO datasets. These findings suggest that LOR may function as a metastasis suppressor in melanoma and hold

promise as a prognostic biomarker for disease progression.

MATERIALS AND METHODS

2.1 Data Sources

Three microarray datasets—GSE65904, GSE59455, and GSE8401—were retrieved from the Gene Expression Omnibus (GEO) database (https://www.ncbi.nlm.nih.gov/geo/) [19-21]. These datasets were selected based on criteria including sample size, data quality, and the inclusion of both primary and metastatic melanoma tissues, to enable the robust identification of consistently differentially expressed genes (DEGs). GSE65904 (GPL10558, Illumina HumanHT-12 V4.0) (Jan 24, 2020) contains 124 metastatic and 16 primary melanoma samples. GSE59455 (GPL8432, Illumina HumanRef-8 WG-DASL v3.0) (Apr 10, 2018) includes 54 metastatic and 22 primary samples. GSE8401 (GPL96, Affymetrix Human Genome U133A Array) (Sep 16, 2019) consists of 52 metastatic and 31 primary tumor samples. All three datasets were generated from microarray-based transcriptomic profiling platforms, and samples were selected to ensure a balanced comparison between primary and metastatic melanoma tissues.

2.2 Identification of Differentially Expressed Genes

DEGs between metastatic and primary melanoma tissues were identified using GEO2R, an online analysis tool based on the limma package in R. Genes were considered differentially expressed if they met the thresholds of adjusted p-value < 0.05 (Benjamini-Hochberg correction) and $|\log_2$ fold change$| > 1$ [22]. GEO2R automatically applies normalization and background correction for each dataset. The InteractiVenn tool (https://www.interactivenn.net/) was used to determine overlapping DEGs across all three datasets [22, 23].

2.3 GO and KEGG Enrichment Analyses

Gene Ontology (GO) enrichment analysis was performed using ShinyGO (v0.82; http://bioinformatics.sdstate.edu/go/). Enriched terms were categorized into biological process (BP), cellular component (CC), and molecular function (MF) domains. Kyoto Encyclopedia of Genes and Genomes (KEGG) pathway analysis was also conducted. Statistical significance was defined as $p < 0.01$ and false discovery rate (FDR) < 0.05 [24-26].

2.4 Protein–Protein Interaction (PPI) Network Construction and Hub Gene Identification

Overlapping DEGs were input into the STRING database (https://string-db.org) to construct a PPI network using a minimum interaction score of 0.4 [27, 28]. The resulting network was imported into Cytoscape (v3.10.2) for visualization and analysis. MCODE (v1.5.1) was used to detect modules with default parameters (degree cutoff = 2, node score cutoff = 0.2, K-Core = 2, max depth = 100). CytoHubba was applied to rank nodes using five algorithms: MCC, Degree, DMNC, NMC, and EPC. Top 10 hub genes were identified, and cross-algorithm consensus analysis yielded three key candidate genes for further validation [29, 30].

2.5 Expression Analysis and Survival Correlation

The GEPIA platform (http://gepia.cancer-pku.cn), based on TCGA and GTEx data, was used to compare gene expression between melanoma and normal skin tissues [31]. The OSdream platform (https://bioinfo.henu.edu.cn/OSdream/) was utilized to assess: differential expression in metastatic vs. non-metastatic melanoma tissues, expression differences in recurrent vs. non-recurrent samples, and the impact of gene expression on metastasis-free survival (MFS) [32]. The p-value reported for the analysis of metastasis-free survival was derived from a log-rank test comparing high versus low expression groups (top vs. bottom quartiles) using the GSE65904 dataset. The hazard ratio (HR) was calculated using univariate Cox regression via OSdream.

2.6. Correlation Analysis

The correlation between selected hub genes and metastasis-related genes was analyzed using expression data from GEO datasets. Pearson correlation coefficients were calculated, and significance was assessed using appropriate statistical tests.

2.7. Statistical Analysis

Two-tailed unpaired t-tests were used to compare gene expression between groups. Multiple testing correction was performed using the Benjamini–Hochberg method (FDR) for DEG and enrichment analysis. For survival analysis, Kaplan–Meier curves, log-rank tests, and univariate Cox regression were used to evaluate metastasis-free survival. Correlation analysis between hub genes and metastasis-related genes was performed using Pearson correlation coefficients. Statistical significance

was set at $p < 0.05$ unless otherwise stated.

RESULTS

3.1 Identification of Common Differentially Expressed Genes (DEGs) Associated with Melanoma Metastasis

To identify potential target genes involved in melanoma metastasis for diagnostic or therapeutic purposes, we analyzed three publicly available gene expression datasets from the Gene Expression Omnibus (GEO): GSE65904, GSE59455, and GSE8401. These datasets contain gene expression profiles from both primary melanoma tissues and metastatic melanoma tissues. Volcano plots were generated to visualize differentially expressed genes (DEGs), with the $\log_2$ fold change on the X-axis and $-\log_{10}$(p-value) on the Y-axis. Significantly upregulated genes are shown in red, downregulated genes in blue, and non-significant genes in gray (Figure 1A–C). The dataset sample distributions were as follows: GSE8401: 31 primary and 52 metastatic samples; GSE59455: 22 primary and 54 metastatic samples; GSE65904: 16 primary and 124 metastatic samples (Figure 1D). To ensure consistency and robustness, we conducted an overlap analysis using a Venn diagram, which identified 37 DEGs shared across all three datasets (Figure 1E). These genes were considered strong candidates for further investigation into their roles in melanoma progression and metastasis.

3.2 Functional Enrichment Analysis Suggests Involvement in Skin Barrier Integrity and Melanoma Metastasis

To explore the biological significance of the 37 common DEGs, we performed Gene Ontology (GO) and Kyoto Encyclopedia of Genes and Genomes (KEGG) enrichment analyses. In the biological process (BP) category, the DEGs were significantly enriched in pathways associated with epidermal development and differentiation, including keratinocyte differentiation, epithelial development, keratinization, skin barrier formation, and regulation of water homeostasis (Figure 2A). These functions are crucial for maintaining skin integrity and may influence tumor dissemination when dysregulated. In the cellular component (CC) category, enriched terms included cornified envelope, keratin filaments, intermediate filament cytoskeleton, lamellar bodies, and multiple extracellular matrix (ECM)-related structures such as collagen-containing ECM and extracellular vesicles (Figure 2B). These components are essential for structural cohesion and tumor microenvironment interactions. In the molecular function (MF) category, DEGs were associated with structural constituents of the skin epidermis and cytoskeleton, as well as peptidase inhibitor activity and enzyme regulator activity (Figure 2C). These functions are often involved in cell adhesion, invasion, and migration, key events in metastasis. KEGG pathway analysis further revealed significant enrichment in the melanogenesis pathway, suggesting that dysregulation of these DEGs may impact melanocyte differentiation and melanoma development (Figure 2D). Taken together, the functional annotation results indicate that the identified DEGs are involved in epidermal barrier regulation, cytoskeletal structure, and signaling pathways relevant to melanoma metastasis. Their altered expression may compromise skin barrier integrity and facilitate tumor invasion and distant dissemination.

3.3 Identification of Key Hub Genes Associated with Melanoma Metastasis

Given that the identified DEGs may play crucial roles in promoting melanoma invasion and metastasis, we next sought to identify the most functionally significant hub genes from this DEG set. To this end, we first constructed a protein-protein interaction (PPI) network using the STRING database (Figure 3A). The resulting network was visualized and further analyzed using Cytoscape software. To identify key functional modules, the MCODE plugin (v1.5.1) was used with default parameters to detect highly interconnected clusters within the PPI network (Figure 3B). Subsequently, we applied the CytoHubba plugin to rank the top hub genes based on five different topological analysis algorithms: MCC, Degree, DMNC, NMC, and EPC (Figure 3C–G). To ensure consistency and robustness, a Venn diagram was used to identify genes that were commonly ranked in the top 10 across all five algorithms. This analysis revealed three consistent hub genes: LOR, KRT6B, and FLG (Figure 3H). To validate their relevance to melanoma biology, we analyzed the expression of these hub genes using the GEPIA platform, which integrates data from TCGA and GTEx. All three genes were significantly downregulated in melanoma tissues compared with normal skin tissues (Figure 4). These findings suggest that the decreased expression of LOR, KRT6B, and FLG may contribute to melanoma development and possibly to its metastatic behavior.

3.4 Clinical Relevance of Hub Genes in Melanoma Metastasis and Prognosis

Since melanoma metastasis and recurrence are primary contributors to therapeutic failure and poor patient prognosis [2, 33], we investigated the clinical relevance of the three hub genes using the TCGA database via the OSdream platform. First, we compared hub gene expression levels between melanoma tissues with and without metastasis. LOR and KRT6B were significantly down-regulated in metastatic tissues, suggesting a potential metastasis-suppressive role. In contrast, FLG expression showed no significant difference (Figure 5A–C). We further assessed whether these hub genes were associated with melanoma recurrence. Expression levels of LOR, KRT6B, and FLG did not differ significantly between recurrent and non-recurrent melanoma tissues, indicating a limited role in recurrence prediction (Figure 5E–G). To evaluate the prognostic value, we performed metastasis-free survival (MFS) analysis using the GSE65904 dataset. Among the three genes, only LOR exhibited a significant prognostic association: patients with high LOR expression (top 25%) had better MFS compared to those with low expression ($p = 0.0466$, HR = 0.5477) (Figure 6B). In contrast, KRT6B ($p = 0.5859$) and FLG ($p = 0.3074$) were not significantly associated with MFS (Figure 6A, C). These results support LOR as a potential metastasis-suppressor gene in melanoma and a promising prognostic biomarker for patient stratification and treatment planning.

3.5 Correlation Analysis Suggests LOR as a Negative Regulator of Melanoma Metastasis

To further explore the biological relevance of LOR in melanoma metastasis, we conducted a correlation analysis between LOR expression and metastasis-related genes using the GSE8401 dataset. This analysis aimed to determine whether LOR is associated with known metastasis-promoting genes, thereby supporting its role as a potential predictive or therapeutic target in melanoma. We selected several metastasis-associated DEGs for comparison. The analysis revealed that LOR expression was negatively correlated with: ADAM12 ($r = –0.2805$, $p = 0.0102$), a gene implicated in extracellular matrix remodeling and tumor invasiveness [34, 35]; ITGA4 ($r = –0.2470$, $p = 0.0241$), a member of the integrin family associated with tumor cell migration and adhesion [6, 36] (Figure 7A, C). Interestingly, LOR showed a strong positive correlation with ITGB3 ($r = 0.8018$, $p = 0.0056$), a gene involved in integrin-mediated signaling and metastatic progression [37, 38] (Figure 7B). This contrasting relationship may reflect gene-specific regulatory networks or context-dependent roles of integrins in melanoma progression. We also examined the association between LOR and CDK1, a cell cycle regulator known to promote melanoma growth and poor prognosis when overexpressed [7, 39, 40]. The analysis showed a significant negative correlation ($r = –0.3966$, $p = 0.0002$), further supporting a potential tumor-suppressive role of LOR in melanoma (Figure 7D). Collectively, these findings suggest that low LOR expression is associated with upregulation of metastasis-promoting genes, reinforcing its putative role as a negative regulator of melanoma progression and metastasis. However, the heterogeneous correlations observed also point to potential sample variability and context-specific interactions, warranting further investigation in larger cohorts and functional studies.

DISCUSSION

Melanoma is an aggressive form of skin cancer arising from melanocytes, and its global incidence has steadily increased over recent decades, particularly among fair-skinned populations exposed to ultraviolet radiation [3]. While early-stage melanoma can be effectively treated by surgical excision, advanced and metastatic melanoma continues to carry a poor prognosis due to its rapid dissemination and limited responsiveness to therapy. Although immune checkpoint inhibitors and BRAF/MEK inhibitors have significantly improved patient outcomes, a substantial proportion of patients ultimately experience disease progression or relapse [2, 41].

Metastasis remains the leading cause of melanoma-related death. The ability to predict and suppress metastasis is therefore critical to improving patient outcomes. Traditional histopathological parameters and clinical staging systems, while informative, are insufficient to stratify metastatic risk in many cases. In this context, transcriptomic profiling and bioinformatic screening of public datasets offer a powerful means to identify key regulators and potential therapeutic targets involved in melanoma dissemination [42, 43]. In this study, we integrated three independent GEO datasets (GSE65904, GSE59455, GSE8401) to identify differentially expressed genes (DEGs) between primary and metastatic melanoma. From 37 consistently altered DEGs, we used PPI net-

work analysis and multi-algorithmic hub gene ranking to identify Loricrin (LOR), Filaggrin (FLG), and Keratin 6B (KRT6B) as key hub genes associated with melanoma progression.

LOR is a major structural component of the cornified envelope, contributing to epidermal differentiation and barrier formation. Though well-characterized in skin disorders like ichthyosis and psoriasis, its role in malignancy has remained largely unexplored [17, 18, 44, 45]. Our study revealed that LOR expression is significantly downregulated in metastatic melanoma and that high LOR expression correlates with improved metastasis-free survival (MFS), suggesting a tumor-suppressive function. Moreover, LOR expression was negatively correlated with ADAM12, ITGA4, and CDK1—key mediators of extracellular matrix degradation, cell adhesion, and proliferation—but positively associated with ITGB3, a molecule involved in integrin signaling and sometimes implicated in immune modulation or adhesion stabilization [6, 35, 38, 39]. These data suggest that LOR may modulate metastatic potential through regulation of epithelial integrity and signaling cascades, and our findings mark the first implication of LOR in melanoma metastasis using transcriptomic analysis.

FLG, another essential barrier-related protein, plays a critical role in keratinocyte terminal differentiation and hydration of the stratum corneum. Loss-of-function mutations in FLG are known to impair epithelial barrier function and are associated with increased risk of HPV-related and skin cancers [46, 47]. In our analysis, FLG was also downregulated in metastatic melanoma tissues, although its expression did not significantly correlate with MFS or recurrence, suggesting a potentially more context-specific role in melanomagenesis or an indirect contribution to tumor microenvironment remodeling.

KRT6B is a stress-induced intermediate filament protein involved in epithelial repair, keratinocyte migration, and re-epithelialization. Its expression is typically elevated in response to skin injury or inflammation and has been linked to cell proliferation and drug resistance in several cancers, including bladder, ovarian, and gastric carcinoma [48-51]. Interestingly, in our study, KRT6B was significantly downregulated in metastatic melanoma samples, suggesting that suppression of KRT6B may reflect a loss of epithelial differentiation or a shift toward a more mesenchymal or stem-like phenotype conducive to invasion. However, unlike LOR, KRT6B did not show a statistically significant correlation with MFS, indicating that its clinical relevance in melanoma metastasis may be more subtle or temporally regulated.

Collectively, our findings highlight a shared pattern of downregulation of epithelial structural genes—LOR, FLG, and KRT6B—in metastatic melanoma, supporting the hypothesis that loss of epithelial integrity contributes to metastatic dissemination. While FLG and KRT6B also exhibited downregulation in metastatic melanoma, their prognostic significance appeared less robust compared to LOR. Of these, LOR appears to have the most consistent prognostic value, with potential as a novel biomarker for metastatic suppression and risk stratification. However, several limitations should be acknowledged. First, this study relies on retrospective transcriptomic datasets generated from different microarray platforms, which may introduce batch effects or technical biases despite normalization. Second, although we identified LOR as significantly associated with metastasis-free survival, we did not stratify samples based on key clinical or molecular subtypes such as BRAF, NRAS, or NF1 mutations, which may influence gene expression profiles and metastatic behavior. Third, the findings are primarily correlative, and the suppressive role of LOR in melanoma progression requires further validation using functional assays in cell lines, animal models, or patient-derived tissues. Additionally, most included datasets were derived from Western populations, which may limit the applicability of our findings to more diverse ethnic cohorts. Future studies should aim to address these limitations by incorporating multi-omics approaches, stratified clinical analyses, and experimental validation to confirm the mechanistic role of LOR in melanoma metastasis.

Beyond its biological implications, the clinical applicability of LOR as a metastasis-suppressive biomarker merits further consideration. The consistent downregulation of LOR in metastatic melanoma, along with its association with improved metastasis-free survival, suggests that LOR expression may be integrated into biomarker panels (e.g., BRAF/NRAS status) to stratify patients based on metastatic risk. Such a panel could complement existing staging systems and potentially guide decisions on surveillance intensity or adjuvant therapy. Moreover, if validated in larger cohorts, LOR may serve as a therapeutic marker for patient selection in clinical trials targeting metastatic pathways. However, the translation of LOR into a clinical biomarker

will require standardized assays—such as immunohistochemistry for tissue detection or qPCR-based quantification—and prospective validation across diverse melanoma subtypes and patient populations. These steps are essential to ensure robustness, reproducibility, and clinical utility in real-world settings.

CONCLUSIONS

In this study, we integrated transcriptomic data from multiple independent GEO datasets and identified LOR, FLG, and KRT6B as key downregulated genes in metastatic melanoma. Among them, LOR showed prognostic significance, correlating with longer metastasis-free survival and inverse expression of metastasis-related genes. These findings suggest LOR as a potential suppressor of melanoma metastasis and a promising prognostic biomarker, though further validation is needed.

ACKNOWLEDGMENTS

This work was supported by Shin Kong Wu Ho-Su Memorial Hospital (2021SKHADR010 and 2022SKHADR009).

REFERENCES

1. Turner, N., O. Ware, and M. Bosenberg, Genetics of metastasis: melanoma and other cancers. Clin Exp Metastasis, 2018. 35(5-6): p. 379-391.
2. Luke, J.J., et al., Targeted agents and immunotherapies: optimizing outcomes in melanoma. Nat Rev Clin Oncol, 2017. 14(8): p. 463-482.
3. Hartman, R.I. and J.Y. Lin, Cutaneous Melanoma-A Review in Detection, Staging, and Management. Hematol Oncol Clin North Am, 2019. 33(1): p. 25-38.
4. Rambow, F., J.C. Marine, and C.R. Goding, Melanoma plasticity and phenotypic diversity: therapeutic barriers and opportunities. Genes Dev, 2019. 33(19-20): p. 1295-1318.
5. Zhu, H., et al., Elevation of ADAM12 facilitates tumor progression by enhancing metastasis and immune infiltration in gastric cancer. Int J Oncol, 2022. 60(5).
6. Fang, T., et al., Lymph Node Metastasis-Related Gene ITGA4 Promotes the Proliferation, Migration, and Invasion of Gastric Cancer Cells by Regulating Tumor Immune Microenvironment. J Oncol, 2022. 2022: p. 1315677.
7. Ravindran Menon, D., et al., CDK1 Interacts with Sox2 and Promotes Tumor Initiation in Human Melanoma. Cancer Res, 2018. 78(23): p. 6561-6574.
8. Wang, W., et al., Zanthoxylum bungeanum seed oil inhibits tumorigenesis of human melanoma A375 by regulating CDC25A/CyclinB1/CDK1 signaling pathways in vitro and in vivo. Front Pharmacol, 2023. 14: p. 1165584.
9. Nichols, E.E., A. Richmond, and A.B. Daniels, Tumor Characteristics, Genetics, Management, and the Risk of Metastasis in Uveal Melanoma. Semin Ophthalmol, 2016. 31(4): p. 304-9.
10. Jin, Y. and X. Qin, Co-expression network-based identification of biomarkers correlated with the lymph node metastasis of patients with head and neck squamous cell carcinoma. Biosci Rep, 2020. 40(2).
11. Ishitsuka, Y., et al., Loricrin and NRF2 Coordinate Cornification. JID Innov, 2022. 2(1): p. 100065.
12. Ishitsuka, Y. and D.R. Roop, Loricrin at the Boundary between Inside and Outside. Biomolecules, 2022. 12(5).
13. Ishitsuka, Y. and D.R. Roop, Loricrin: Past, Present, and Future. Int J Mol Sci, 2020. 21(7).
14. Kim, B.E., et al., Particulate matter causes skin barrier dysfunction. JCI Insight, 2021. 6(5).
15. Catunda, R.Q., et al., Loricrin and Cytokeratin Disorganisation in Severe Forms of Periodontitis. Int Dent J, 2023. 73(6): p. 862-872.
16. Cosgarea, I., et al., Melanoma secretion of transforming growth factor-beta2 leads to loss of epidermal AMBRA1 threatening epidermal integrity and facilitating tumour ulceration. Br J Dermatol, 2022. 186(4): p. 694-704.
17. AMBRA1 and loricrin as a test to identify low-risk early-stage melanoma. Br J Dermatol, 2024. 190(4): p. e46.
18. Ewen, T., et al., Validation of epidermal AMBRA1 and loricrin (AMBLor) as a prognostic biomarker for nonulcerated American Joint Committee on Cancer stage I/II cutaneous melanoma. Br J Dermatol, 2024. 190(4): p. 549-558.
19. Landi, M.T., et al., Gene expression signature of cigarette smoking and its role in lung adenocarcinoma

development and survival. PLoS One, 2008. 3(2): p. e1651.
20. Lu, T.P., et al., Identification of regulatory SNPs associated with genetic modifications in lung adenocarcinoma. BMC Res Notes, 2015. 8: p. 92.
21. Sanchez-Palencia, A., et al., Gene expression profiling reveals novel biomarkers in nonsmall cell lung cancer. Int J Cancer, 2011. 129(2): p. 355-64.
22. Barrett, T., et al., NCBI GEO: archive for functional genomics data sets--update. Nucleic Acids Res, 2013. 41(Database issue): p. D991-5.
23. Heberle, H., et al., InteractiVenn: a web-based tool for the analysis of sets through Venn diagrams. BMC Bioinformatics, 2015. 16(1): p. 169.
24. Ge, S.X., D. Jung, and R. Yao, ShinyGO: a graphical gene-set enrichment tool for animals and plants. Bioinformatics, 2020. 36(8): p. 2628-2629.
25. Kanehisa, M., et al., KEGG: integrating viruses and cellular organisms. Nucleic Acids Res, 2021. 49(D1): p. D545-D551.
26. Luo, W. and C. Brouwer, Pathview: an R/Bioconductor package for pathway-based data integration and visualization. Bioinformatics, 2013. 29(14): p. 1830-1.
27. Szklarczyk, D., et al., The STRING database in 2011: functional interaction networks of proteins, globally integrated and scored. Nucleic Acids Res, 2011. 39(Database issue): p. D561-8.
28. Szklarczyk, D., et al., The STRING database in 2023: protein-protein association networks and functional enrichment analyses for any sequenced genome of interest. Nucleic Acids Res, 2023. 51(D1): p. D638-D646.
29. Shannon, P., et al., Cytoscape: a software environment for integrated models of biomolecular interaction networks. Genome Res, 2003. 13(11): p. 2498-504.
30. Chin, C.H., et al., cytoHubba: identifying hub objects and sub-networks from complex interactome. BMC Syst Biol, 2014. 8 Suppl 4(Suppl 4): p. S11.
31. Tang, Z., et al., GEPIA: a web server for cancer and normal gene expression profiling and interactive analyses. Nucleic Acids Res, 2017. 45(W1): p. W98-W102.
32. Li, H., et al., OSdream: An online survival and differential analysis tool of recurrence and metastasis of pan-cancers. Genes Dis, 2025. 12(4): p. 101446.
33. Li, B., et al., Programmed Intermittent Epidural Bolus at Different Intervals Combined with Patient-controlled Epidural Analgesia on Body Temperature during Labour Analgesia. J Coll Physicians Surg Pak, 2020. 30(5): p. 463-466.
34. Wang, R., et al., Hypoxia-inducible factor-dependent ADAM12 expression mediates breast cancer invasion and metastasis. Proc Natl Acad Sci U S A, 2021. 118(19).
35. Xu, J., et al., ADAM12 promotes clear cell renal cell carcinoma progression and triggers EMT via EGFR/ERK signaling pathway. J Transl Med, 2023. 21(1): p. 56.
36. Nurzat, Y., et al., Identification of Therapeutic Targets and Prognostic Biomarkers Among Integrin Subunits in the Skin Cutaneous Melanoma Microenvironment. Front Oncol, 2021. 11: p. 751875.
37. Li, F., et al., Platelet-derived extracellular vesicles inhibit ferroptosis and promote distant metastasis of nasopharyngeal carcinoma by upregulating ITGB3. Int J Biol Sci, 2022. 18(15): p. 5858-5872.
38. Cheng, C., et al., Positive feedback regulation of lncRNA TPT1-AS1 and ITGB3 promotes cell growth and metastasis in pancreatic cancer. Cancer Sci, 2022. 113(9): p. 2986-3001.
39. Aly, A.A., et al., Design, Synthesis, and Molecular Docking of Paracyclophanyl-Thiazole Hybrids as Novel CDK1 Inhibitors and Apoptosis Inducing Anti-Melanoma Agents. Molecules, 2020. 25(23).
40. Luan, H., et al., Exploration and validation of metastasis-associated genes for skin cutaneous melanoma. Sci Rep, 2022. 12(1): p. 13002.
41. Knackstedt, T., et al., Malignant Melanoma: Diagnostic and Management Update. Plast Reconstr Surg, 2018. 142(2): p. 202e-216e.
42. Chen, B., et al., Screening and identification of potential biomarkers and therapeutic drugs in melanoma via integrated bioinformatics analysis. Invest New Drugs, 2021. 39(4): p. 928-948.
43. Xie, R., et al., Identification of Core Genes and Pathways in Melanoma

Metastasis via Bioinformatics Analysis. Int J Mol Sci, 2022. 23(2).
44. Ishitsuka, Y. and D.R. Roop, The Epidermis: Redox Governor of Health and Diseases. Antioxidants (Basel), 2021. 11(1).
45. Abbotto, E., et al., SIRT6 pharmacological inhibition delays skin cancer progression in the squamous cell carcinoma. Biomed Pharmacother, 2023. 166: p. 115326.
46. Skaaby, T., et al., Associations of filaggrin gene loss-of-function variants and human papillomavirus-related cancer and pre-cancer in Danish adults. PLoS One, 2014. 9(6): p. e99437.
47. Vanderbeck, K., et al., Filaggrin expression via immunohistochemistry in basal cell carcinoma and squamous cell carcinoma. J Cutan Pathol, 2021. 48(7): p. 877-883.
48. Ricciardelli, C., et al., Keratin 5 overexpression is associated with serous ovarian cancer recurrence and chemotherapy resistance. Oncotarget, 2017. 8(11): p. 17819-17832.
49. Lim, S.C., K.R. Parajuli, and S.I. Han, Keratin 6, induced by chronic cisplatin exposure, confers chemoresistance in human gastric carcinoma cells. Oncol Rep, 2019. 42(2): p. 797-804.
50. Wang, X., et al., eIF6 modulates skin wound healing by upregulating keratin 6B. Stem Cells Transl Med, 2024. 13(11): p. 1101-1112.
51. Nargis, N., D.A. Sens, and A.A. Mehus, Knockdown of Keratin 6 Within Arsenite-Transformed Human Urothelial Cells Decreases Basal/Squamous Expression, Inhibits Growth, and Increases Cisplatin Sensitivity. Cells, 2024. 13(21).

FIGURE AND FIGURE LEGENDS

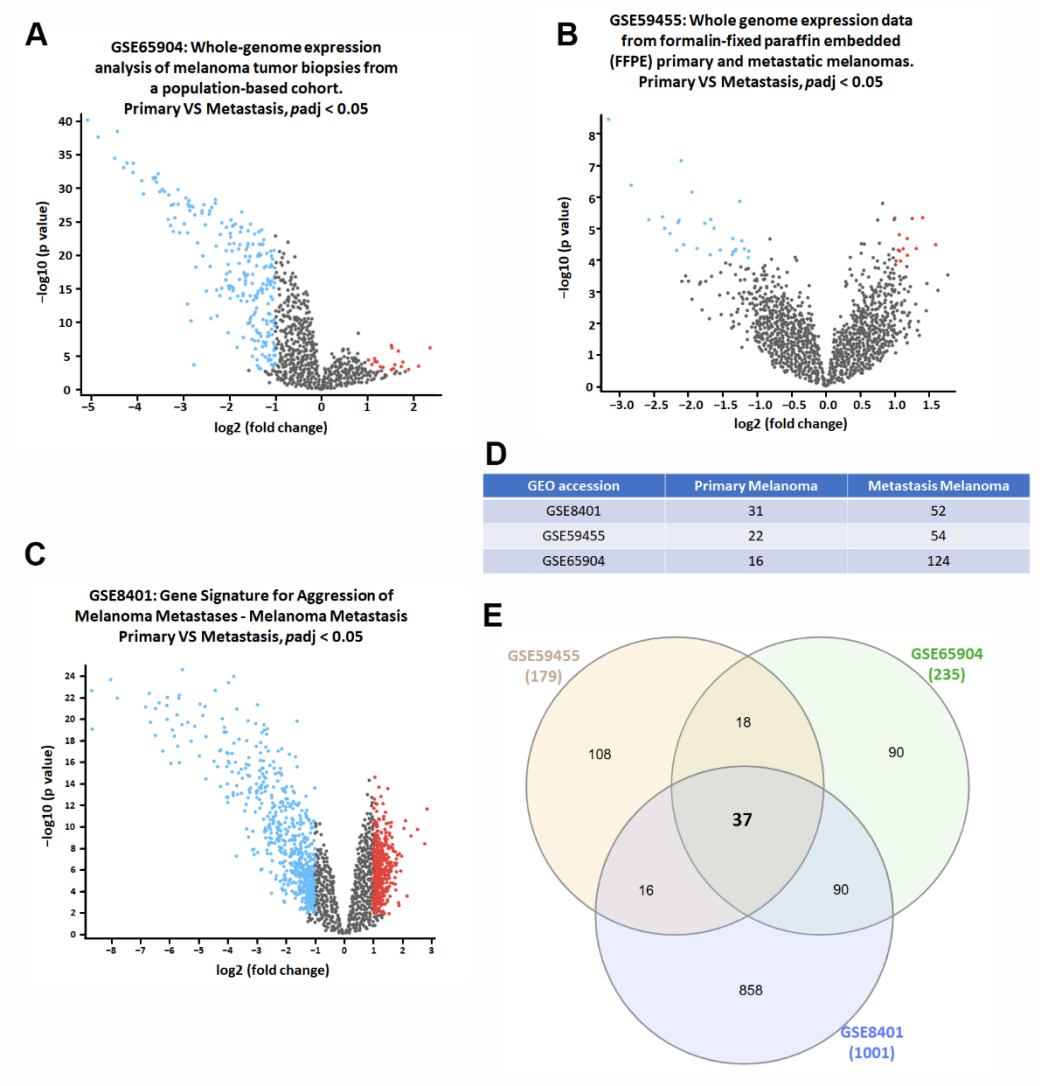

GEO accession	Primary Melanoma	Metastasis Melanoma
GSE8401	31	52
GSE59455	22	54
GSE65904	16	124

Figure 1. Identification of differentially expressed genes (DEGs) in melanoma datasets. (A–C) Volcano plots of DEGs between metastatic and primary melanoma tissues in the GSE8401, GSE59455, and GSE65904 datasets. Red dots: significantly upregulated genes; blue dots: significantly downregulated genes; gray dots: non-significant. (D) The list showing sample distribution across datasets. (E) Venn diagram showing 37 overlapping DEGs among the three datasets.

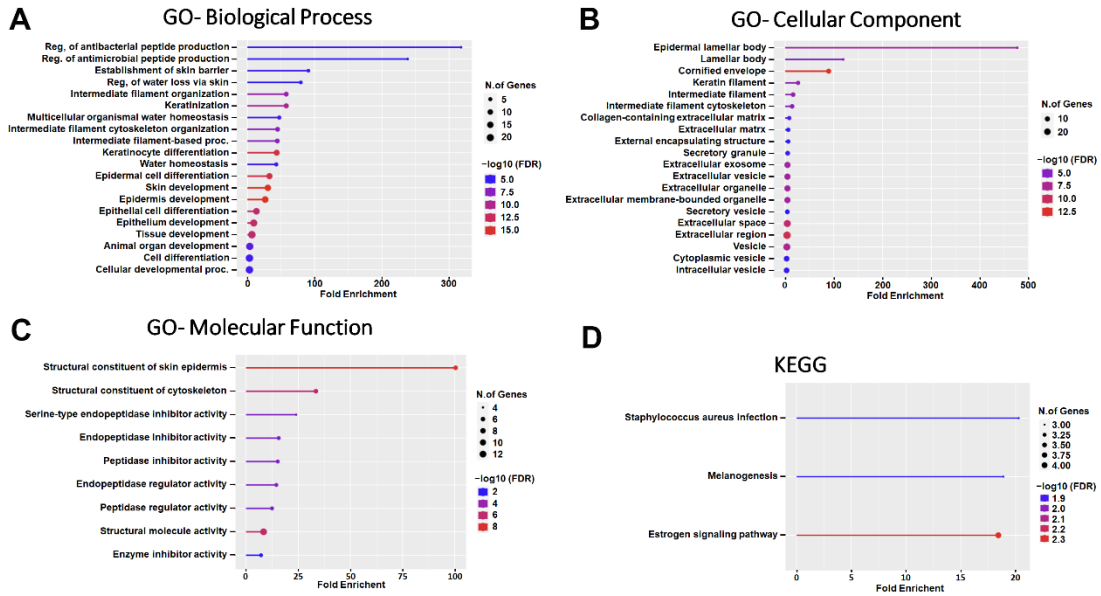

Figure 2. GO and KEGG enrichment analysis of DEGs. (A) Biological process (BP) terms of DEGs after GO analysis. (B) Cellular component (CC) terms of DEGs after GO analysis. (C) Molecular function (MF) terms of DEGs after GO analysis. (D) KEGG pathway of DEGs after KEGG analysis.

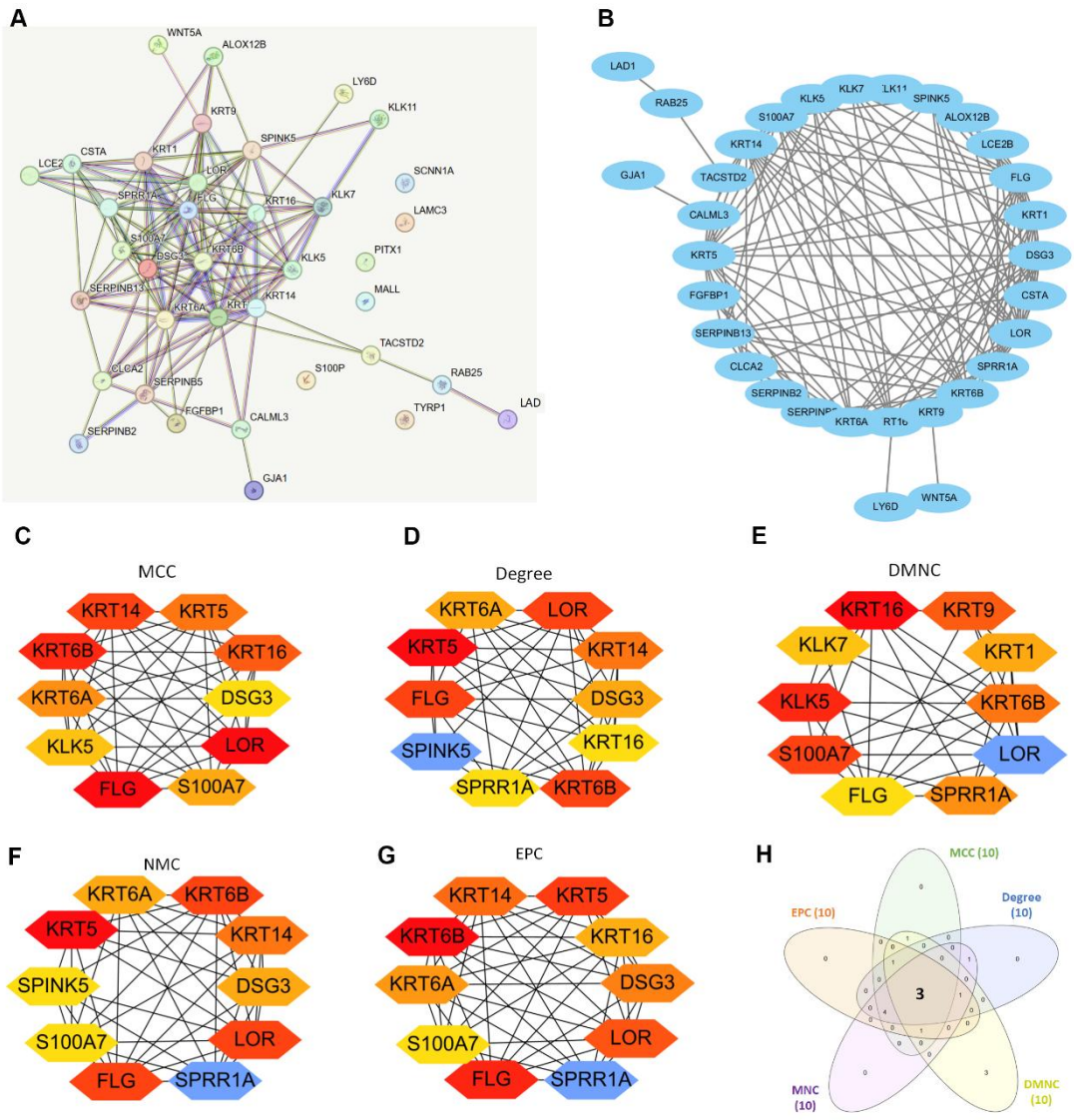

Figure 3. Identification of hub genes from PPI network analysis. (A) PPI network of overlapping DEGs constructed using STRING database. (B) MCODE module analysis showing densely connected clusters. (C–G) Top 10 ranked hub genes identified using five CytoHubba algorithms (MCC, Degree, DMNC, NMC, EPC). (H) Venn diagram showing three consensus hub genes shared across all algorithms.

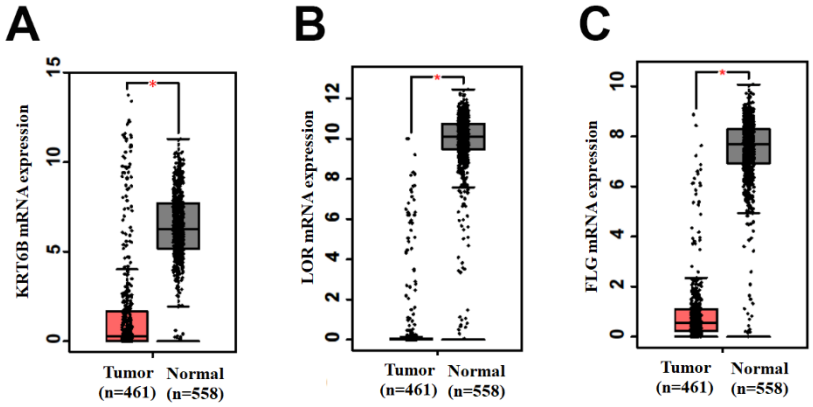

Figure 4. Expression levels of hub genes in melanoma versus normal tissues. (A-C) GEPIA platform analysis showing the expression in melanoma compared to normal skin tissues: keratin 6B (KRT6B), loricrin (LOR), and filaggrin (FLG). *p < 0.05.

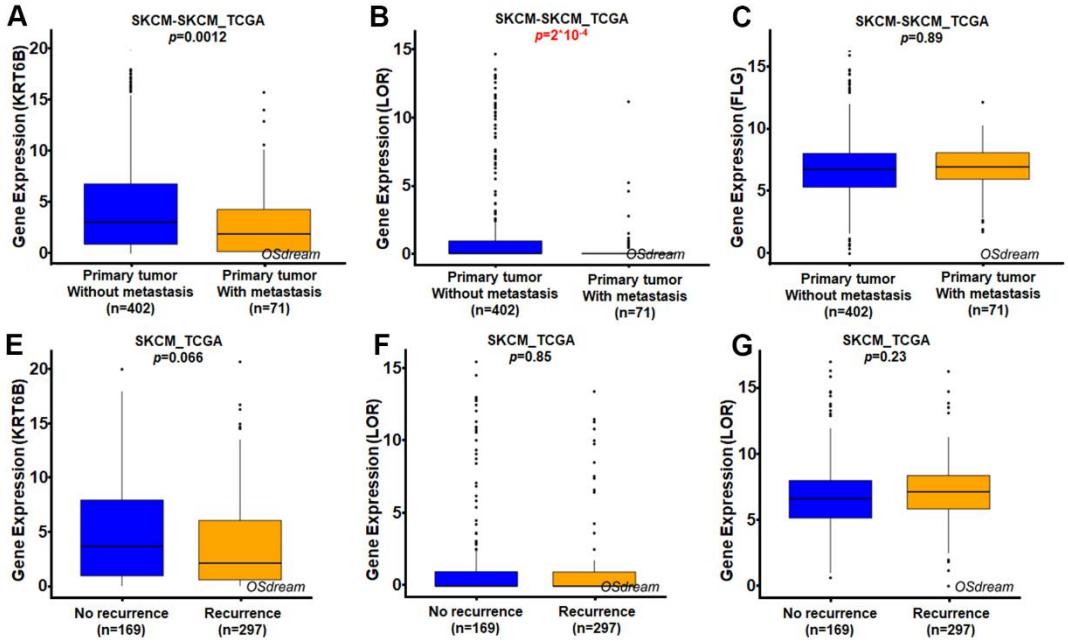

Figure 5. Expression of hub genes in recurrence/metastasis TCGA melanoma dataset. (A–C) Expression of KRT6B, LOR, and FLG in melanoma with or without metastasis. (D–F) Expression levels in recurrent versus non-recurrent melanoma tissues. *p < 0.05.

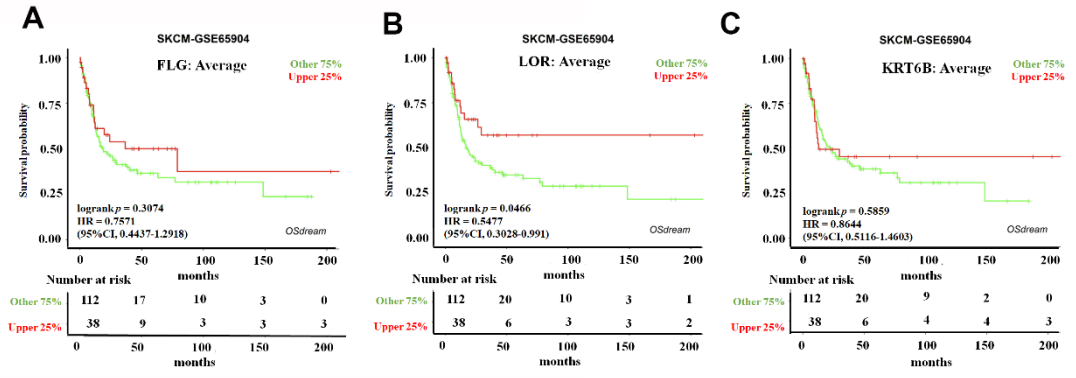

Figure 6. Kaplan–Meier analysis of metastasis-free survival (MFS) based on hub gene expression in the GSE65904 cohort. Patients were stratified into two groups based on gene expression levels: the top 25% were defined as the high-expression group, and the remaining 75% as the low-expression group. Kaplan–Meier survival curves were used to compare MFS between the two groups for KRT6B, LOR, and FLG. Log-rank test p-value and hazard ratios (HR) are shown on the plots. *$p < 0.05$.

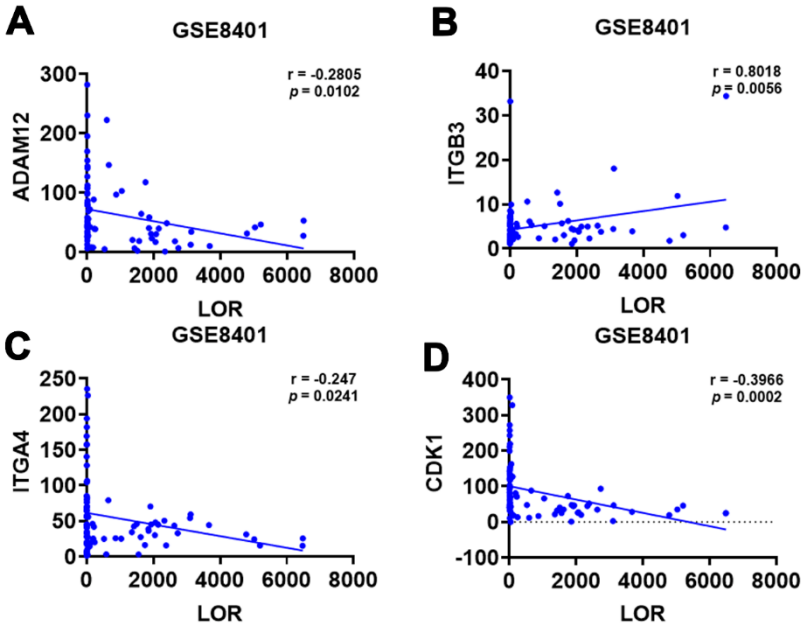

Figure 7. Correlation of LOR expression with metastasis-related genes in melanoma. Scatter plots depict the correlation between LOR expression and the expression of ADAM12, ITGA4, CDK1, and ITGB3 in the GSE8401 dataset. Pearson correlation coefficients (r) and corresponding two-tailed p-values are indicated. *$p < 0.05$.

Multi-Dataset Transcriptomic Analysis Uncovers Loricrin as a Key Suppressor of Melanoma Metastasis

整合多重轉錄體資料揭示 Loricrin 為黑色素瘤轉移之關鍵抑制因子

張耀仁 [1,2]　張琮銘 [2]　林致凡 [3]　劉如芳 [3,4,]　張繼仁 [5,6*]

中文摘要

背景：黑色素瘤是一種高度侵襲性的皮膚癌，一旦發生轉移，預後極差。鑑別具有轉移抑制潛力的生物標誌物，對於改善臨床治療成效至關重要。**材料與方法**：本研究整合三個 GEO 資料庫數據集（GSE65904、GSE59455、GSE8401），分析轉移性與原發性黑色素瘤組織間的差異表現基因（DEGs）。藉由 STRING、Cytoscape（MCODE、CytoHubba）及 Venn 分析進行 GO/KEGG 功能富集、蛋白質交互作用（PPI）網絡建構與核心基因篩選。臨床相關性則透過 GEPIA 與 OSdream 平台加以驗證。**結果**：共鑑定出 37 個重疊的 DEGs，富集於角質形成細胞分化與上皮屏障功能等相關途徑。其中，loricrin（LOR）、角蛋白 6B（KRT6B）與 filaggrin（FLG）在黑色素瘤中表現一致下調，並被鑑定為核心基因。LOR 表現量與較長的無轉移存活期（metastasis-free survival, p = 0.0466）相關，且其表現與 ADAM12、ITGA4、CDK1 等促轉移基因呈負相關。此結果顯示 LOR 可能具轉移抑制作用。**結論**：LOR 為一潛在預測黑色素瘤轉移與疾病進展的生物標誌物，具臨床預後與治療開發應用價值。

關鍵字：黑色素瘤、轉移、Loricrin（LOR）、生物資訊學、差異表現基因（DEGs）

[1] 新光醫療財團法人新光吳火獅紀念醫院整型外科，台北市 111045 臺灣

[2] 臺北醫學大學口腔醫學院牙體技術學系，台北市 11031，臺灣

[3] 新光醫療財團法人新光吳火獅紀念醫院轉譯醫學中心，台北市 111045，臺灣

[4] 臺北醫學大學口腔醫學院口腔衛生學系，台北市 11031，臺灣

[5] 輔仁大學醫學系，新北市 24205，臺灣

[6] 新光醫療財團法人新光吳火獅紀念醫院小兒外科，台北市 111045，臺灣

[*]通訊作者：張繼仁　電子信箱 m002008@ms.skh.org.tw

Submitted September 08, 2024.
Final version accepted November 16, 2024.

Cite as: Chi-Jung Chang, Ming-Dar Tsai
Spontaneous Regression of Lumbar Disc Herniation with Adjacent Level Disc Herniation– A Case Presentation and Literatures Review
Fu-Jen Journal of Medicine 23(3): 33-39, 2025.
DOI: 10.53106/181020932025092303003

Case Report

Spontaneous Regression of Lumbar Disc Herniation with Adjacent Level Disc Herniation– A Case Presentation and Literatures Review

Chi-Jung Chang[1,2], Ming-Dar Tsai[1,3,*]

[1] Section of Neurosurgery, Department of Surgery, Shin Kong Wu Ho-Su Memorial Hospital, Taipei City, Taiwan

[2] Department of Neurosurgery, Neurological Institute, Taipei Veterans General Hospital

[3] School of Medicine, Fu-Jen Catholic University, Xinzhuang District, New Taipei City, Taiwan

*Corresponding author. E-mail address: tmdhealer@gmail.com (Ming-Dar Tsai)

ABSTRACT

Lumbar disc herniation is a common condition, but adjacent segment disease (ASD) without prior surgery is rare. We aimed to reveal the chance of spontaneous regression with adjacent level disc herniation by presenting a case of a 36-year-old woman who experiencing chronic low back pain and subsequent radiation pain in both lower extremities. She did not undergo surgical intervention at first. With different complaint, she returned to clinic. Magnetic resonance imaging (MRI) showed spontaneously regressed lumbar herniated disc and a newly developed disc herniation at upward adjacent level without surgical intervention. Regression of the lumbar disc herniation is not a rare condition. For patients that has no absolute indication to surgery, conservative treatment could be attempted first. However, limited research exists on ASD in patients without prior surgery, making it difficult to conclude whether this patient's condition is ASD or an unrelated disc degeneration event.

Keywords: Herniated disc, Spontaneous regression, Low back pain, Lumbar radiculopathy, Adjacent Segment Disease

INTRODUCTION

Lumbar disc herniation is a common problem that neurosurgeon would face in the clinic. Lumbar disc herniation might compress nerve roots, leading to radiculopathy or even cauda equina syndrome. Patients with symptomatic lumbar disc herniation can be treated either non-surgically or surgically. Most of the symptoms of lumbar herniated disc would be relieved within 6 weeks [1]. In addition, it was observed on some of these patients, that the herniated part of the intervertebral disc shrank or even disappeared, through imaging examinations such as magnetic resonance imaging and computerized tomography [1-3]. However, it

was rare to see adjacent segment disease in a patient without receiving operation. Adjacent segment disease involves new symptoms at spinal levels adjacent to a previously treated site, often arising from increased mechanical stress after fusion surgery. Although fusion is commonly associated with ASD, studies suggest it can also occur following procedures like laminectomy and laminoplasty, with varying reoperation rates. Here we present a case of spontaneous complete regression of lumbar herniated intervertebral disc with a new herniated disc a level above in a 36- year-old woman and review literature to explain this phenomenon.

CASE REPORT

A 36-year-old woman without any underlying disease complained of chronic low back pain for several years. The symptoms became more apparent, and she developed radiation pain in both lower extremities, with the right side being more predominant. Upon physical and neurological examination, the straight leg raising test was positive at an angle of 30 degrees on the right side. Lumbar spinal magnetic resonance imaging (MRI) revealed a ruptured disc at L5/S1 (Figure 1), causing compression of the right S1 root. We suggested surgical intervention; however, she preferred conservative treatment.

Five years later, she presented to our outpatient clinic again, this time complaining of numbness in the right big toe for a few months. Follow-up MRI (Figure 2.) revealed the resolution of the previous L5/S1 ruptured disc, but a new herniated disc at the L4/5 level causing L5 radiculopathy was identified. Despite being advised to undergo surgical intervention, she still preferred conservative treatment. Eventually, she was lost to follow-up.

This study was approved by Institutional Ethics Review Board (Permission reference: 20240906R).

DISCUSSION

Since the year of 1984 when the first case of regression under non-surgical treatment was reported, regression without surgical intervention has become a consideration when physicians plan treatment for symptomatic lumbar disc herniation [2].

In 1996, Saal and his colleagues discussed different classification that might have impact on the nature course of lumbar disc herniation, including its type, location, associated anatomical, histochemical factors, clinical characteristics, and individual factors on the nature course of lumbar disc herniation [3].

Since then, many papers were published to figure out the regression rate of symptomatic lumbar disc herniation. A systemic review in 2020 analyzed 38 articles [4]. The pooled incidence of regression was 63%. The issue is determining the appropriate timing for surgical intervention. A study included in this meta-analysis revealed no regression within 45 days [7]. Therefore, the author indicated that we should not expect the symptoms subsided within 6 weeks after onset. There were 7 included studies that showed similar regression incidence to the pooled incidence of regression [8-14]. The shortest follow-up time among these 7 studies was 4 months [4,14]. The average follow-up period of the other six studies was 10.5 months [4,8-13]. Based on the results, the authors suggest a follow-up timeline that consists of the time points 4 and 10.5 months after onset when deciding whether to perform surgery.

Besides incidence and timing of regression, many researchers aimed to find out which type of the disc herniation has the highest regression rate [3,5,6]. The classification of disc herniation includes bulge, protrusion, extrusion, and sequestration. A review pointed out that macrophage regulation of inflammatory mediators, matrix metalloproteinases, and specific cytokines in intervertebral disc is necessary for the spontaneous reabsorption of lumbar disc herniation [5]. Since extrusion and sequestration of lumbar disc herniation can squeeze out of the epidural space, it sets up conditions conducive for macrophage infiltration and neovascularization [5]. A recent meta-analysis found that the pooled overall incidence of disk resorption was 70.39%, with the highest rate observed for disc sequestration at 87.77%, followed by extrusion at 66.91%, disc protrusion at 37.53%, and disc bulge at 13.33%, respectively [6].

Another interesting issue in this case is adjacent segment disease. Our patient developed a bulging disc at the level adjacent to the previously herniated one. Adjacent segment disease is primarily defined as the presentation of new symptoms referable to an adjacent level after undergoing surgical intervention, particularly following fusion. It is thought to arise from increased biomechanical demands on segments adjacent to a fused area, which may transmit greater forces and lead to degeneration. [15]

Laminectomy has been considered an option to reduce the incidence rate of adjacent

segment disease compared to fusion. Nevertheless, a review article published in 2013 pointed out that adjacent segment disease can occur not only after spinal fusion but also following laminectomy. Reoperation rates after laminectomy for spinal stenosis without spondylolisthesis range from 2.7% to 36% over 5 to 10 years. Furthermore, laminoplasty could also cause adjacent segment disease. Notably, there was a significant difference in reoperation rates compared to laminectomy. [16]

Until now, there have been very few articles describing the phenomenon of a patient suffering from adjacent segment disease without operation. The natural progression of lumbar degenerative disease involves the gradual drying out of all lumbar discs, although the rate of degeneration varies among different spinal segments. [16] More evidence is needed to determine whether our patient has adjacent segment disease or if this is an isolated event.

CONCLUSION

Spontaneous regression of the lumbar disc herniation is not a rare condition. For patients that has no absolute indication to surgery, conservative treatment could be attempted first. Patient such as the case presented above suffering from disc sequestration might have the greatest chance of spontaneous resorption. In addition, we could also pay attention on its adjacent segment to see if there is any degenerative change. The question of whether non-surgical treated disc herniation could easily lead to accelerated degeneration of adjacent segments is worth exploring.

REFERENCES

1. Schoenfeld AJ, Weiner BK. Treatment of lumbar disc herniation: evidence-based practice. Int J Gen Med. 2010;3:209–14.
2. Guinto FC Jr, Hashim H, Stumer M. CT demonstration of disk regression after conservative therapy. AJNR Am J Neuroradiol. 1984;5(5):632–3.
3. Saal JA, Saal JS, Herzog RJ. The natural history of lumbar intervertebral disc extrusions treated nonoperatively. Spine (Phila Pa 1976). 1990;15(7):683–6.
4. Wang, Y., Dai, G., Jiang, L. et al. The incidence of regression after the non-surgical treatment of symptomatic lumbar disc herniation: a systematic review and meta-analysis. BMC Musculoskelet Disord 21, 530 (2020).
5. https://doi.org/10.1186/s12891-020-03548-z
6. Yu, P., Mao, F., Chen, J. et al. Characteristics and mechanisms of resorption in lumbar disc herniation. Arthritis Res Ther 24, 205 (2022).
7. https://doi.org/10.1186/s13075-022-02894-8
8. Zou T, Liu XY, Wang PC et al. Incidence of Spontaneous Resorption of Lumbar Disc Herniation: A Meta-analysis. Clin Spine Surg. 2024 Jul 1;37(6):256-269. doi: 10.1097/BSD.0000000000001490. Epub 2023 Jul 31. PMID: 37559207.
9. Santilli V, Beghi E, Finucci S. Chiropractic manipulation in the treatment of acute back pain and sciatica with disc protrusion: a randomized double-blind clinical trial of active and simulated spinal manipulations. Spine J. 2006;6(2):131–7.
10. Ahn SH, Ahn MW, Byun WM. Effect of the transligamentous extension of lumbar disc herniations on their regression and the clinical outcome of sciatica. Spine (Phila Pa 1976). 2000;25(4):475–80.
11. Delauche-Cavallier MC, Budet C, Laredo JD, Debie B, Wybier M, Dorfmann H, et al. Lumbar disc herniation: computed tomography scan changes after conservative treatment of nerve root compression. Spine. 1992;17(8):927–33.
12. Bozzao A, Gallucci M, Masciocchi C, Aprile I, Barile A, Passariello R. Lumbar disk herniation: MR imaging assessment of natural history in patients treated without surgery. Radiology. 1992;185(1):135–41.
13. Matsubara Y, Kato F, Mimatsu K, Kajino G, Nakamura S, Nitta H. Serial changes on MRI in lumbar disc herniations treated conservatively. Neuroradiology. 1995;37(5):378–83.
14. Komori H, Shinomiya K, Nakai O, Yamaura I, Takeda S, Furuya K. The natural history of herniated nucleus pulposus with radiculopathy. Spine (Phila Pa 1976). 1996;21(2):225–9.
15. Bush K, Cowan N, Katz DE, Gishen P. The natural history of sciatica associated with disc pathology. A prospective study with clinical and independent radiologic follow-up. Spine (Phila Pa 1976). 1992;17(10):1205–12.
16. Iwabuchi M, Murakami K, Ara F, Otani K, Kikuchi S. The predictive factors for the resorption of a lumbar disc herniation

on plain MRI. Fukushima J Med Sci. 2010;56(2):91–7.

17. Alan S. Hilibrand, Matthew Robbins. Adjacent segment degeneration and adjacent segment disease: the consequences of spinal fusion? The Spine Journal, Volume 4, Issue 6, supplement (2004) Pages S190-S194, ISSN 1529-9430. https://doi.org/10.1016/j.spinee.2004.07.007.
18. Kristen E. Radcliff, Christopher K. Kepler, Andre Jakoi et. al. Adjacent segment disease in the lumbar spine following different treatment interventions. The Spine Journal, Volume 13, Issue 10 (2013) Pages 1339-1349, ISSN 1529-9430. https://doi.org/10.1016/j.spinee.2013.03.020.

FIGURE AND FIGURE LEGEND

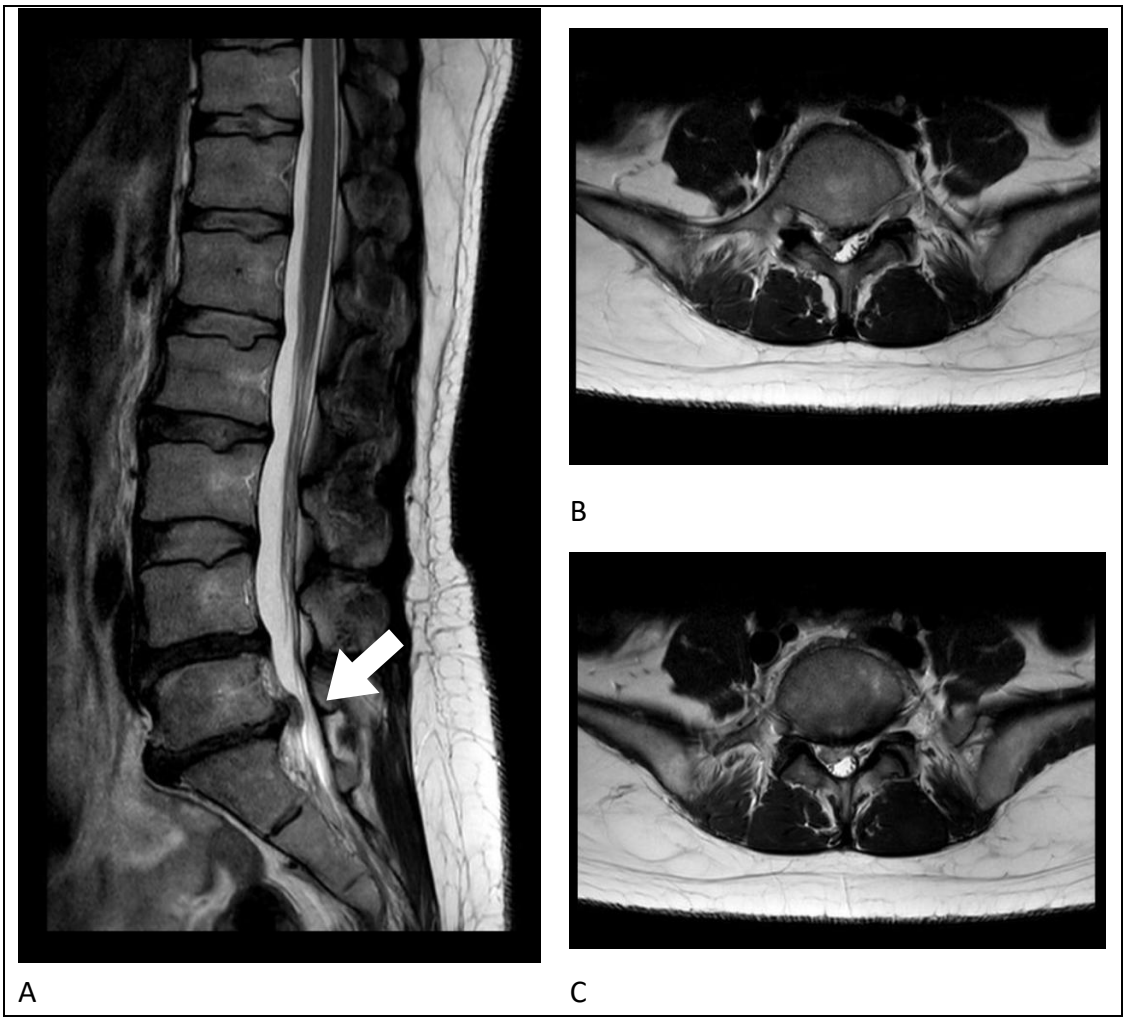

Figure 1. Lumbar spinal MRI obtained before first presentation. A. Sagittal view of lumbar spine. A ruptured disc at L5/S1 protruded to canal. B. Axial view of the affected level (L5/S1). The ruptured disc resulting in S1 root compression. C. Axial view of the affected level (L5/S1).

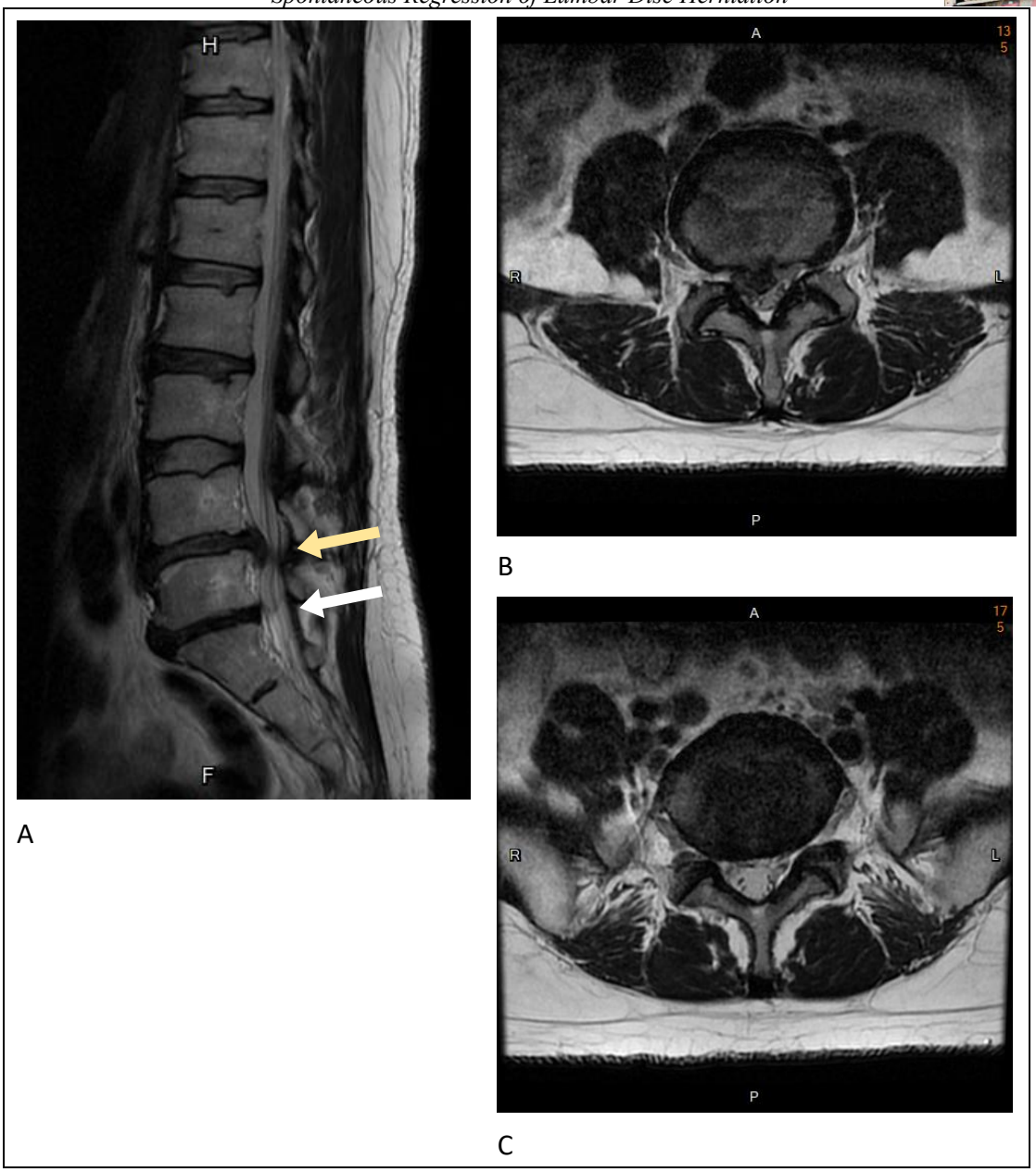

Figure 2. Lumbar spinal MRI obtained after second presentation. A. Sagittal view of lumbar spine. A ruptured disc protruded to canal at L4/5. B. Axial view of the L4/5 level (yellow arrow in Figure2A.). The ruptured disc resulting in right L5 root compression. C. Axial view of the L5/S1 level (White arrow in Figure 2A). The protruded disc regressed spontaneously

Spontaneous Regression of Lumbar Disc Herniation with Adjacent Level Disc Herniation– A Case Presentation and Literatures Review

病例報告及文獻回顧：腰椎椎間盤突出的自發性消退伴隨鄰近節次椎間盤突出

張起榮 [1,2,] 蔡明達 [1,3,*]

中文摘要

腰椎間盤突出是一種常見的疾病，但在無手術病史的情況下出現鄰近節段疾病（ASD）則較為罕見。我們旨在透過介紹一例 36 歲女性的案例來揭示自發性消退緩解但卻衍生出鄰近節段椎間盤突出的機率。她經歷了慢性腰痛以及隨後的雙下肢放射痛。最初她沒有接受手術介入。隨著症狀的改變，她再次回到門診。磁振造影（MRI）顯示，原腰椎間盤突出在沒有手術介入的情況下自發性緩解，但在上方鄰近節段出現新的椎間盤突出。腰椎間盤突出的自發性緩解並非罕見情況。對於沒有絕對手術適應症的患者，臨床上可以先嘗試保守治療。然而，目前對於無手術病史的患者出現 ASD 的研究非常有限，因此很難判斷該患者的情況是 ASD 還是單純獨立的椎間盤退化現象。

關鍵字：椎間盤突出、自發性消退、下背痛、腰椎神經根病變、鄰近節段病變

[1] 新光醫療財團法人新光吳火獅紀念醫院 神經外科

[2] 臺北榮民總醫院神經醫學中心神經外科

[3] 天主教輔仁大學醫學院醫學系

[*]通訊作者：蔡明達　電子信箱 tmdhealer@gmail.com

Submitted February 18, 2025.
Final version accepted March 20, 2025.

Cite as: Ching-Wen Huang, Shu-Han Huang, Gong-Yau Chu Rapid-onset de novo Crohn's Disease following Ixekizumab therapy in patient with chronic plaque psoriasis: A Case Report and Literature Review
Fu-Jen Journal of Medicine 23(3): 40-44, 2025.
DOI: 10.53106/181020932025092303004

Case Report

Rapid-onset de novo Crohn's Disease following Ixekizumab therapy in patient with chronic plaque psoriasis: A Case Report and Literature Review

Ching-Wen Huang[1], Shu-Han Huang[2], Gong-Yau Chu[3,4,*]

[1] Department of Diagnostic Radiology, Shin-Kong Wu Ho-Su Memorial Hospital, Taipei 11101, Taiwan, R.O.C.

[2] Department of Diagnostic Radiology, Shin-Kong Wu Ho-Su Memorial Hospital, Taipei 11101, Taiwan, R.O.C.

[3] Department of Dermatology, Shin-Kong Wu Ho-Su Memorial Hospital, Taipei 11101, Taiwan.

[4] School of Medicine, College of Medicine, Fu Jen Catholic University, New Taipei, 242062, Taiwan.

* Corresponding author. E-mail address: aguest122@hotmail.com.tw (Gong-Yau Chu)

ABSTRACT

Psoriasis is a chronic inflammatory dermatosis. Ixekizumab is a monoclonal antibody that targets interleukin 17A (IL-17A) and indicated for plaque psoriasis. In 2024, a study analyzed the long-term safety of ixekizumab in patients with psoriasis(6892 cases) and identified 31 cases of inflammatory bowel disease (IBD; 0.5%, incidence rate 0.2 per 100 PY), of which 18 were cases of ulcerative colitis (0.3%, incidence rate 0.1 per 100 PY) and 13 of Crohn's disease (CD; 0.2%, incidence rate 0.7 per 100 PY). However, subgroup analysis of Japanese patients in a phase III study on ixekizumab uncovered no cases of IBD. The literature suggest that CD following ixekizumab therapy is uncommon, especially in Asian patients. Herein, we report the case of a Taiwanese patient who developed rapid-onset de novo CD following ixekizumab therapy for chronic plaque psoriasis. Ixekizumab therapy was administered as per the instruction sheet, and his symptoms appeared 2 days following the 2nd dose of ixekizumab. Due to the rarity, we report this case to highlight the importance of adverse event. Early detection and diagnosis result in a good outcome. Physicians should be alert to its possibility. Careful history taking of gastrointestinal symptoms is recommended before and after anti-IL-17 therapy.

Keywords: psoriasis, Crohn's disease, biologics, ixekizumab, IL-17

INTRODUCTION

Psoriasis is a chronic inflammatory dermatosis, which is a systemic disorder associated with arthritic, psychological, cardiovascular, and metabolic complications. [1] According to the Taiwan National Health Insurance Research Database (NHIRD) from 2006 to 2017, the prevalence of psoriasis increased from 0.18% to 0.86%, but its incidence rate remained constant at 62–65 per 100,000 person-years (PY).[1] This result suggests that new medications, such as various biologic agents, have improved the life expectancy of patients with psoriasis.[1] However, the immunomodulatory effects and long-course treatments of biologic therapies for psoriatic patients may lead to adverse outcomes arising from inadequate immune-mediated reactions.[2]

Ixekizumab is a monoclonal antibody that targets interleukin 17A (IL-17A).[2] In 2024, a study analyzed the long-term safety of ixekizumab in patients with psoriasis including 6892 patients from 17 randomized controlled trials (RCTs); the analysis identified 31 cases of inflammatory bowel disease (IBD; 0.5%, incidence rate 0.2 per 100 PY), of which 18 were cases of ulcerative colitis (0.3%, incidence rate 0.1 per 100 PY) and 13 of Crohn's disease (CD; 0.2%, incidence rate 0.7 per 100 PY).[2] However, subgroup analysis of Japanese patients in a phase III study on ixekizumab uncovered no cases of ulcerative colitis or CD.[3] Overall, results in the literature suggest that CD following ixekizumab therapy is uncommon, especially in Asian patients. Herein, we report the case of a Taiwanese patient who developed rapid-onset de novo CD following ixekizumab therapy for chronic plaque psoriasis.

CASE REPORT

A 28-year-old Taiwanese man with a history of psoriasis vulgaris presented to the emergency department with acute-onset abdominal pain and bloody diarrhea. His vital signs were stable, and no additional symptoms or signs of infection were present. He denied a personal or family history of IBD and was a teetotaler and nonsmoker. Ixekizumab therapy was administered as per the instruction sheet. Symptoms appeared 2 days following the 2nd dose of ixekizumab. No other systemic drug exposure was noted.

His white blood cell count was 9500/mm3 and C-reactive protein level was 0.28 mg/dL. Other blood test results were within normal limits. A stool test revealed occult blood without pus, and no abnormal bacteria were found in the stool culture. Colonoscopy revealed some large ulcers and small aphthous-like ulcers in the ileocecal valve and ascending colon (Figure. 1). Samples were taken from these ulcers for mycobacterial culture and pathology tests. Histopathology results indicated colonic tissue with fissuring ulcers, granulation tissue formation, and proliferation of collagen fibers. Focal distortion of architecture and transmural lymphocytic infiltration were noted. Moderate lymphoplasma cells and some neutrophil infiltration were detected in the stroma (Figure. 2). Acid-fast staining and mycobacterial culture yielded negative results.

The patient received a diagnosis of CD on the basis of his clinical presentation, colonoscopy findings, histological analysis, and laboratory results. According to his history, biologics agents induced CD was highly suspected. Ixekizumab was stopped, and the patient was treated with mesalazine at a daily dose of 2 g. His symptoms started improving after 1 week of mesalazine treatment. No recurrence was noted within a 7-month follow-up period.

DISCUSSION

CD is a chronic and relapsing inflammatory disorder of the intestinal tract and commonly affects the terminal ileum and proximal colon. The symptoms of CD are diverse and dependent on location and severity. The common clinical presentations include diarrhea, abdominal pain, weight loss, and fatigue. [4] The risk factors include having an affected first-degree relative, cigarette smoking, antibiotic exposures and ultra-processed foods. [4] Nevertheless, the concordance rate for CD only reaches 50% in monozygotic twins. [4] This result emphasizes the importance of non-genetic factors in patients with CD. The possible mechanism for the pathogenesis of CD is recognized to be multifactorial with the hypotheses of the interactions between genetic, environmental, and microbial factors resulting in the induction of dysregulated immune responses in genetically susceptible groups.[4] The incidence rates of CD were relatively low in adults from Asian countries.[5] A retrospective study based on data in Taiwan reported that the annual incidence of CD was 0.47/100,000 persons in 2015, which was extremely low compared with that in other countries.[5]

IL-17 is a proinflammatory cytokine secreted by various mimmune cells, including innate lymphoid cells (ILC), mucosal-associated invariant T cells (MAIT) and T helper cells [6], and blockade of IL-17 reveals clinical improvement in psoriasis and multiple immune-mediated diseases [6]. The expression of IL-17 was reported

to be higher in the intestinal mucosa of patients with IBD. Therefore, the inhibition of IL-17 pathway was thought to have a beneficial therapeutic effect in treating IBD. [6] Though interestingly, clinical trials involving patients with IBD suggest that anti-IL-17 agents have failed to display clinical benefits and even cause exacerbations of clinical presentations in patients with CD. [6] Furthermore, new onset of IBD patients following treatment with IL-17 blockers have been recorded in both clinical researches and postmarketing drug surveillance. [6] As a result, IL-17 may have paradoxical effects in the pathogenesis of IBD.[6] This may be because blockade of IL-17 can weaken immunity against pathogens and induce epithelial barrier breakdown.[6] Moreover, inhibiting IL-17 can modify the cytokine environment and disrupt the expression of IL-22, which promotes mucosal healing.[6] But, the rarity of new-onset IBD cases following the treatment with IL-17 inhibitors and the presence of several zero-event clinical trials suggest that interpretation of the association between anti-IL-17 antibodies and IBD needs caution.[6] In 2019, a systematic review and meta-analysis including 16,690 patients from 38 RCTs who were treated with anti-IL-17 agents revealed that the risk of new-onset IBD was statistically nonsignificant.[6]

However, a real-world study using data from the US Food and Drug Administration's Adverse Event Reporting System database from 2015 to 2022 demonstrated that IL-17 inhibitor treatment was associated with exacerbation of IBD and new-onset IBD.[7] The onset time of symptoms was mainly within 6 months of therapy, and 18.5% of cases developed symptoms within one month. The median time to onset of IBD symptoms was 2.9 months. The median age was 42 years. The typical presentations included diarrhea (90.9%), abdominal pain (57.6%), bloody diarrhea (51.5%), and fever (36.4%). Cessation of biological agent plus treatment could result in complete clinical remission for those IBD patients in association with IL-17 blockers. The clinical courses were different from the other CD patients with chronic and relapsing presentations. The median time to remission after IL-17 inhibitor discontinuation was 4 weeks, and 20% of patients subsided within 2 weeks.

There is limited literature for rapid-onset de novo CD following ixekizumab therapy in Asian patients. Due to the rarity, we report this case to highlight the importance of adverse event. Early detection and diagnosis result in a good outcome. Physicians should be alert to its possibility. Careful history taking of gastrointestinal symptoms is recommended before and after anti-IL-17 therapy. Additional cases should be reported to enhance postmarket pharmacovigilance.

*The study was approved by the Institutional Review Board on 2024-9-20 (IRB No.: 20240910R)

REFERENCES

1. Ireny Y K Iskandar, Teng-Chou Chen, Li-Chia Chen, Meng-Sui Lee, Yen-Yun Yang, Ting-Chun Wang, etc. Incidence, Prevalence, and Mortality of People with Psoriasis and Psoriatic Arthritis in Taiwan: A Nationwide Cohort Study. Acta Derm Venereol. 2022; 102: 1962.
2. Atul Deodhar, Andrew Blauvelt, Mark Lebwohl, Meghan Feely, Andris Kronbergs, Nadezhda Eberhart, etc. Long-term safety of Ixekizumab in adults with psoriasis, psoriatic arthritis, or axial spondyloarthritis: a post-hoc analysis of final safety data from 25 randomized clinical trials. Arthritis Res Ther. 2024; 26: 49.
3. Efficacy and safety of ixekizumab treatment for Japanese patients with moderate to severe plaque psoriasis, erythrodermic psoriasis and generalized pustular psoriasis: Results from a 52-week, open-label, phase 3 study (UNCOVER-J). J Dermatol. 2017 Apr; 44:355-362.
4. Michael Dolinger, Joana Torres, Severine Vermeire. Crohn's disease. Lancet. 2024; 403:1177-1191.
5. Satimai Aniwan, Priscila Santiago, Edward V Loftus Jr, Sang Hyoung Park. The epidemiology of inflammatory bowel disease in Asia and Asian immigrants to Western countries. United European Gastroenterol J. 2022; 10:1063-1076.
6. Akihiro Yamada, Jingzhou Wang, Yuga Komaki, Fukiko Komaki, Dejan Micic, Atsushi Sakuraba. Systematic review with meta-analysis: risk of new onset IBD with the use of anti-interleukin-17 agents. Aliment Pharmacol Ther. 2019; 50:373-385.
7. Zhenzhen Deng, Shengfeng Wang, Cuifang Wu1, Chunjiang Wang. IL-17 inhibitor-associated inflammatory bowel disease: A study based on literature and database analysis. Front Pharmacol. 2023; 14: 1124628.
8. .

FIGURE AND FIGURE LEGENDS

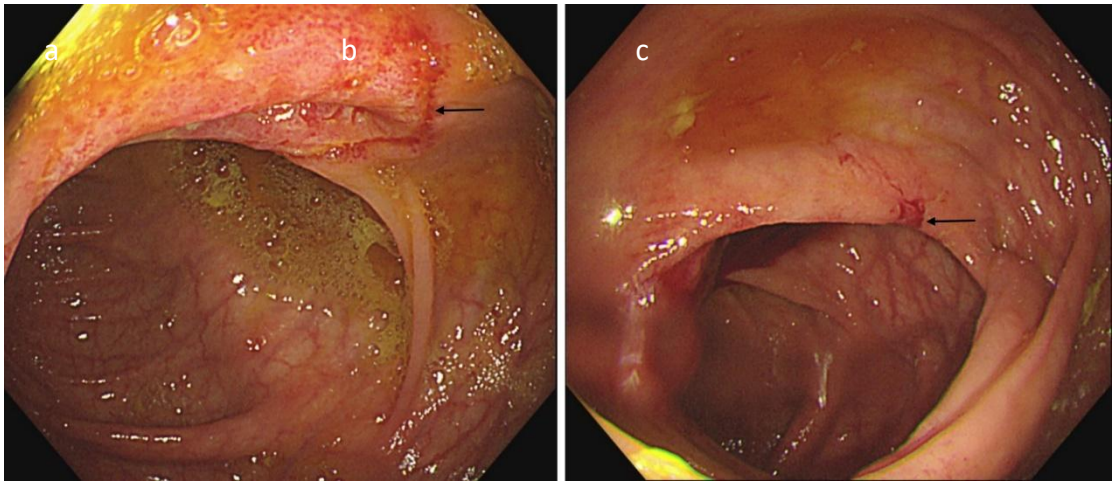

Figure 1. Colonoscopy image revealing multiple large ulcers and small aphthous-like ulcers.

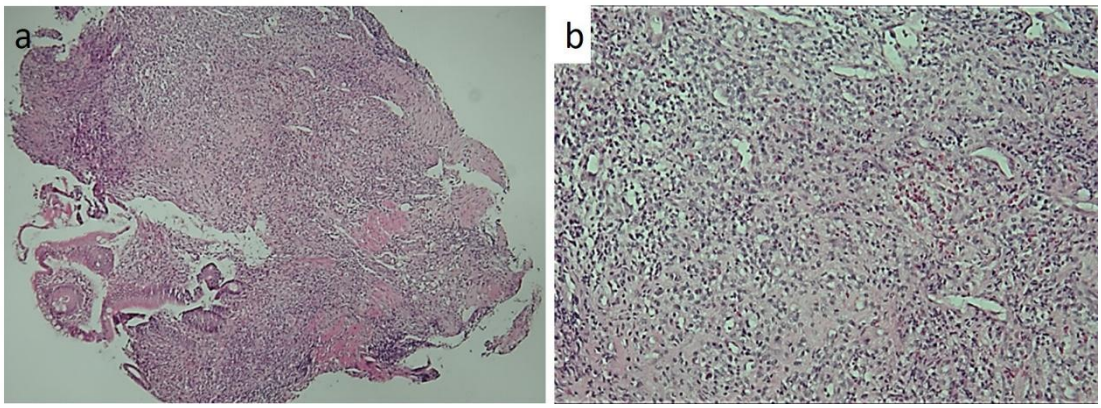

Figure 2. a: Examination of colonic mucosal biopsy specimens in low-power view indicating fissuring ulceration of the colonic mucosa with epithelial damage and structural changes. Focal areas of transmural inflammation are noted.
b: Examination of colonic mucosal biopsy specimens in high-power view indicating granulation tissue formation with active infiltration of inflammatory cells.

Rapid-onset de novo Crohn's Disease following Ixekizumab therapy in patient with chronic plaque psoriasis: A Case Report and Literature Review

使用 Ixekizumab 後快速發生克隆氏症的斑塊型乾癬病人病例報告

黃敬雯[1]　黃書瀚[2]　朱宮瑤[3,4,*]

中文摘要

乾癬是慢性發炎的皮膚疾病，生物製劑為近代廣泛使用的治療。Ixekizumab 為一種單株抗體，是針對與乾癬致病機轉的 IL-17 開發的藥物，已經核准並且用於臨床。在 2024 年一篇長期安全性報告中，有提及此藥物可能會誘發發炎性腸道疾病，雖然發生率極低，潰瘍性結腸炎為千分之三，克隆氏症為千分之二，但是依然值得注意。發炎性腸道疾病在亞洲族群發生率是低於歐美族群，並且此藥物在臨床實驗時，納入的亞洲族群日本人並無任何人罹病。但是我們以 Ixekizumab 治療一名 28 歲無任何過去病史及家族史的乾癬病人後，卻產生克隆氏症，其發生速度快，依仿單使用在第二劑施打完二天，就發生血便腹痛症狀，經大腸鏡檢查並切片證實，病人也在馬上停藥治療後，一周後緩解，七個月皆無復發，此一罕見使用 Ixekizumab 後快速發生克隆氏症病例報告，顯示臨床醫師早期發現，早期治療期，可獲得良好預後。

關鍵字：乾癬、克隆氏症、生物製劑

[1] 新光吳火獅紀念醫院放射診斷科

[2] 新光吳火獅紀念醫院病理檢驗科

[3] 新光吳火獅紀念醫院皮膚科

[4] 天主教輔仁大學醫學院醫學系

[*]通訊作者：朱宮瑤　電子信箱 aguest122@hotmail.com.tw

Fu-Jen Journal of Medicine

Mission and Goals

The Fu-Jen Journal of Medicine (FJJM) is a peer-reviewed journal which aims to enhance research quality of staffs in the College of Medicine, Fu Jen Catholic University. The journal publishes original investigations across a wide range of medical disciplines including original research articles in basic and clinical sciences, case reports, review articles, brief reports, and letter to the editor. FJJM is now issued by the Center of Medical Education in the College of Medicine, Fu Jen Catholic University. To promote journal quality, the manuscript submitted to FJJM after August first 2015 has to be prepared in English to meet the international standards.

Issue Date	December 01 2003
Publication Date	September 30 2025
Institution	College of Medicine, Fu Jen Catholic University
Honorable publisher	Yi-Chen Lan
Publisher	Jun-Hou Liao
Editor-in-chief	Ke-hsin Chueh
Associate Editors	Jian-Hong Yeh, Yu-Wen Lin, Vin-chi Wang Shih-Chang Lin

Telephone	(02) 2905-3477
Address	Center for Medical Education, College of Medicine, Fu Jen Catholic University No. 510 Zhongzheng Rd, Xinzhuang Dist., New Taipei City, 24205 Taiwan

輔仁大學醫學院
College of Medicine Fu Jen Catholic University

TEL : +886-2-2905 3477
E-mail : fjjm@mail.fju.edu.tw
No.510,Zhongzheng Rd, Xinzhuang Dist
New Taipei City 24205, Taiwan.(R.O.C)

http:// cme.mc.fju.edu.tw